



Cite this: *Mater. Horiz.*, 2022, 9, 1356

## Environment tolerant, adaptable and stretchable organohydrogels: preparation, optimization, and applications

Qionglin Ding,<sup>a</sup> Zixuan Wu,<sup>a</sup> Kai Tao,<sup>b</sup> Yaoming Wei,<sup>a</sup> Weiyan Wang,<sup>a</sup> Bo-Ru Yang,<sup>a</sup> Xi Xie <sup>a</sup> and Jin Wu <sup>\*a</sup>

Multiple stretchable materials have been successively developed and applied to wearable devices, soft robotics, and tissue engineering. Organohydrogels are currently being widely studied and formed by dispersing immiscible hydrophilic/hydrophobic polymer networks or only hydrophilic polymer networks in an organic/water solvent system. In particular, they can not only inherit and carry forward the merits of hydrogels, but also have some unique advantageous features, such as anti-freezing and water retention abilities, solvent resistance, adjustable surface wettability, and shape memory effect, which are conducive to the wide environmental adaptability and intelligent applications. This review first summarizes the structure, preparation strategy, and unique advantages of the reported organohydrogels. Furthermore, organohydrogels can be optimized for electro-mechanical properties or endowed with various functionalities by adding or modifying various functional components owing to their modifiability. Correspondingly, different optimization strategies, mechanisms, and advanced developments are described in detail, mainly involving the mechanical properties, conductivity, adhesion, self-healing properties, and antibacterial properties of organohydrogels. Moreover, the applications of organohydrogels in flexible sensors, energy storage devices, nanogenerators, and biomedicine have been summarized, confirming their unlimited potential in future development. Finally, the existing challenges and future prospects of organohydrogels are provided.

Received 19th November 2021,  
Accepted 25th January 2022

DOI: 10.1039/d1mh01871j

rsc.li/materials-horizons

### 1. Introduction

Flexible electronics, through the integration of mechanical flexibility and electrical properties in devices, have been well developed in the past decade due to their tremendous application prospects in next-generation portable electronics.<sup>1–5</sup> Various stretchable materials, including elastomers, hydrogels, ionogels,

<sup>a</sup> State Key Laboratory of Optoelectronic Materials and Technologies and the Guangdong Province Key Laboratory of Display Material and Technology, School of Electronics and Information Technology, Sun Yat-sen University, Guangzhou 510275, China. E-mail: wujin8@mail.sysu.edu.cn

<sup>b</sup> The Ministry of Education Key Laboratory of Micro and Nano Systems for Aerospace, Northwestern Polytechnical University, Xi'an, 710072, P. R. China



Qionglin Ding

Qionglin Ding received her BE and MA in micro-electronics from Lanzhou University. She is currently a PhD student in the School of Electronics and Information Technology, Sun Yat-sen University. Her current research interest is stretchable sensing devices.



Zixuan Wu

Zixuan Wu received his BE from Sun Yat-Sen University. He is currently pursuing his PhD degree at Sun Yat-Sen University. His research interest includes gas/humidity sensors and stretchable electronics.

and organogels, have been successively developed and used in practice due to their unique properties. Elastomers, such as polydimethylsiloxane (PDMS),<sup>6</sup> ecoflex, polymethyl methacrylate (PMMA),<sup>7</sup> thermoplastic polyurethanes (TPU),<sup>8</sup> and various rubber materials,<sup>9</sup> are elastic materials based on high molecular polymer networks and have excellent strength and toughness. However, most elastomers do not possess high strain capacity and conductivity, and are usually used as packaging materials and flexible substrates. Research studies show that dispersing polymer networks in different dispersion media is beneficial to construct gel materials with distinct (desired) characteristics. Hydrogels usually consist of physically and/or chemically crosslinked 3D polymer networks dispersed in a large amount of water. This makes the hydrogels display both solid-like mechanical properties (strength, stretchability, and toughness) and a liquid-like transport capacity (ions and nutrients).<sup>10,11</sup> The combination of the unique network structure and composition endows hydrogels with exceptional stretchability, toughness, biocompatibility, and high ionic conductivity,<sup>12,13</sup> making them potential candidates in diverse fields, including wearable and implantable electronics, bionic sensors, actuators, soft robotics, tissue engineering, flexible energy storage devices, *etc.*<sup>14–17</sup>

Nevertheless, the practical applications of hydrogels are still limited by many problems. First, compared with natural load-bearing materials such as tendons, conventional hydrogels have limited mechanical stiffness and low toughness, which are caused by the sparse, homogeneous, and microscale 3D network structure.<sup>18,19</sup> Second, there has always been a dilemma of the trade-off between the mechanical performance and ionic conductivity in conventional hydrogels. Unfortunately, higher mechanical properties often require a denser network structure, and this will inhibit ion transport and sacrifice part of the ionic conductivity.<sup>20–22</sup> Then, wide environmental adaptability is particularly important for flexible electronic devices for their applications in different environments, even in sub-zero, dry, and underwater environments. However, due to the presence of a large amount of water, the freezing-induced hardening issue at sub-zero temperatures and evaporation-induced structural dehydration will inevitably occur in the hydrogel,

which will eventually lead to the loss of its functionality.<sup>23,24</sup> Finally, multiple functions, such as self-healing, adhesiveness, transparency, and antibacterial properties, are rarely achieved in conventional hydrogels synchronously.<sup>25–27</sup> Due to these inevitable issues, it is of great practical significance to develop anti-freezing and anti-drying hydrogels with excellent mechanical properties and tunable functionalities. Ionogels use ionic liquids as dispersion media and exhibit outstanding stability and mechanical characteristics, and have great potential to be used in flexible electronics, owing to the good ionic conductivity, non-volatility, non-flammable properties, and electrochemical stability of ionic liquids.<sup>28–31</sup> However, ionic liquids are relatively expensive and toxic, which are not conducive to applications in biological tissues and large-scale production. Besides, organogels are obtained by mixing polymer chains with organic solution and gelators, which exhibit good viscoelasticity and thermoplasticity.<sup>32,33</sup> Generally, various properties of these soft materials can be easily regulated and implemented by changing their composition, structure, concentration, *etc.*

To date, although remarkable progress has been made in the development of various pristine stretchable materials, their actual applications are always limited by the intrinsic problems of a single system. There is an urgent need to develop gel materials that have excellent mechanical properties, conductivity, and stability in various environments simultaneously. Taking into account both advantages and drawbacks of individual components, the hybrids of these stretchable materials have been widely utilized and have significant advantages in performance optimization by integrating the advantages of each component.<sup>34</sup> For example, the incorporation of ionic liquids makes hydrogels not only moderately conductive but also highly stretchable.<sup>3,35,36</sup> Alternatively, compared with pristine hydrogels, the binary system of hydrogels and elastomers shows higher mechanical strength and also maintains excellent stretchability.<sup>37–40</sup> In addition, due to the entirely opposite physiochemical properties of organogels and hydrogels, it is highly desirable to obtain organogel–hydrogel hybrids with a wealth of unique properties. Correspondingly, Guo *et al.* formally proposed the concept of organohydrogels by gelling cellulose and poly(vinyl alcohol) (PVA) in a mixed solvent



**Yaoming Wei**

*Yaoming Wei received his BE from Chongqing University in 2019. He is currently pursuing his Master's degree at Sun Yat-Sen University. His research interests focus on gas sensors and stretchable electronics.*



**Jin Wu**

*Jin Wu received his PhD degree from Nanyang Technological University in 2014. After obtaining his PhD in 2014, he continued to work in SMART program in Nanyang Technological University as a postdoctoral research fellow. Since 2017, he works as an associate professor at the School of Electronics and Information Technology, Sun Yat-sen University. His research interest includes hydrogel-based sensors, flexible and stretchable electronics, *etc.**

of dimethylformamide (DMF) and water.<sup>41</sup> Interestingly, this organohydrogel exhibited relatively high stability in various solvents without dissolution, shrinkage, or swelling, so that the enzyme electrodes based on it could work in various liquid media without being limited by the solubility of the analytes. Over the past few decades, a lot of efforts have been devoted to the preparation, performance optimization, and application expansion of organohydrogels. As a consequence, various types of organohydrogels have been developed, and they are a good alternative to traditional hydrogels through the elimination of the electro-mechanical performance deterioration caused by freezing, dehydration, or swelling of hydrogels under specific harsh conditions, showing good frost resistance, moisture retention, and solvent resistance. Based on the incomparable multi-environmental tolerance of other gel materials, it can be widely used in soft robotics, tissue engineering, and stretchable electronics even in harsh environments, such as cold winters, dry deserts, and liquid environments.<sup>15,16,42,43</sup> In addition, the thermoplastic organogel domains and the stable hydrogel elastic network in organohydrogels that feature a binary cooperative phase result in thermally-induced variable mechanical properties, which are expected to serve as promising smart materials to suit a variety of applications.<sup>44–47</sup>

Beyond this, with the broadened application of flexible materials, new functional requirements for organohydrogels have increased sharply, such as self-adhesiveness, self-healing, antibacterial properties, and transparency. To implement these goals, functionalized organohydrogels can be achieved through the modification of specific functional monomers and delicate composition, and molecular and structural engineering.

Nevertheless, it remains a great challenge to develop organohydrogels with all these functions simultaneously, owing to some trade-off dilemma. Herein, a systematic and comprehensive introduction and summary of organohydrogels are presented (Fig. 1). Firstly, the preparation methods and unique characteristics of two different types of organohydrogels are introduced in detail, including heteronetwork and homogeneous organohydrogels. Then, the research significance and strategies for further optimization and additional giving of electro-mechanical properties and various functionalities in organohydrogels reported previously are summarized and discussed, respectively, which will undoubtedly play an indispensable role in the development of multifunctional organohydrogels in the future. Finally, the representative applications of organohydrogels in different fields are described in detail, mainly focusing on sensing devices, energy storage devices, nanogenerators, and biomedicine.

## 2. Configuration design for organohydrogels

### 2.1. Classification and preparation

Organohydrogel is currently a very typical and common gel material, and its construction generally requires two processes to occur: a polymerization process in which organic monomers are interconnected to form long molecular chains and a cross-linking process in which molecular chains are cross-linked to form a network. During the gelation of the polymer network, two cross-linking mechanisms are mainly involved.<sup>48</sup> One is physical cross-linking, and the gel network formed accordingly is



Fig. 1 Schematic illustration of the classification, preparation, functionalization, and application of organohydrogels.

mainly cross-linked by non-covalent bonds. To date, the repeated freezing and thawing process is the most common method to obtain physically cross-linked hydrogels through the formation of hydrogen bonds and crystalline domains.<sup>24,49</sup> Representatively, PVA-based hydrogels can be directly obtained by dissolving PVA powder in a solvent and then performing several freeze-thaw cycles, and their mechanical properties can be adjusted by the number of freeze-thaw cycles.<sup>50,51</sup> As for PVA-based organohydrogels, only one freeze-thaw cycle can form a stable gel.<sup>49,52</sup> This is due to the formation of large numbers of hydrogen bonds and the induction of PVA crystallization after the introduction of organic agents, thus increasing the cross-linking points, which greatly improves the production efficiency. Besides, gelatin-based hydrogels can be obtained by heating the gelatin in a solvent to dissolve and dissociate into coil-like chains, and then the gelatin molecules rearrange into triple helix structures through hydrogen bonding and hydrophobic interaction after cooling down, which is also another common method to obtain a physically cross-linked network.<sup>53,54</sup> Specifically, the preparation of these polymer networks is completely green and pollution-free as no polymerization reaction occurs.<sup>55</sup>

Another cross-linking mechanism is called chemical cross-linking. In this regard, conventional radical polymerization is deployed to construct a strong covalent cross-linking network as a typical method, requiring a well-designed polymerization step. In the polymer precursor solution, the polymer monomer, initiator, and cross-linker need to be included. In addition, the occurrence of phase transition requires induction from external stimuli, such as heat,<sup>56</sup> pH,<sup>57</sup> light,<sup>58–60</sup> or redox.<sup>61,62</sup> Among them, photopolymerization and thermal polymerization are the most common, and the corresponding photoinitiator (2-hydroxy-2-methylpropiophenone<sup>63,64</sup> and 2,2'-diethoxyacetophenone (DEAP)<sup>65</sup>) and thermal initiator (ammonium persulfate (APS)<sup>66–68</sup> and 2,2'-azobis(2-methylpropionitrile) (AIBN)<sup>69</sup>) are used. Chemical cross-linkers such as *N,N*-methylene bisacrylamide (MBA) are the key to gelation, and the gelation of different polymers often requires different types of cross-linking agents, which is adverse to the expansion of polymer types in gel materials.<sup>64,69,70</sup> Apart from these surfactants, solid materials such as nanoclays,<sup>71</sup> MXenes,<sup>72</sup> and silica nanoparticles<sup>73</sup> have also been reported as cross-linkers or to accelerate the gelation process. However, compared to physical cross-linking, the preparation of these chemical reagents is relatively complicated and costly, and the residual reagents after polymerization may cause contamination and damage to biological tissues, which is not conducive to the biocompatibility of the gel materials and their application in biomedicine.<sup>63,65,66</sup> Beyond this, partial free radical polymerization generally needs to be carried out under oxygen-free conditions, and the complex polymerization process limits its large-scale production and practical application.<sup>74,75</sup>

According to the different components in the organohydrogel, there are mainly two different types of organohydrogels that can be constructed: one is a heteronetwork organohydrogel, in which hydrophilic and hydrophobic polymer networks interpenetrate each other or two immiscible phases are independently distributed in the matrix at microscale dimensions.<sup>76,77</sup> The other

is a homogeneous organohydrogel containing one or more homogeneous hydrophilic polymer networks in a binary-solvent (organic/water) system. So far, various organic solvents for the construction of organohydrogels have been developed, mainly including glycerol (Gly), ethylene glycol (EG), and dimethyl sulfoxide (DMSO).

As for heteronetwork organohydrogels, there are mainly three synthetic methods that have been developed in the past decade (Fig. 2). For example, Gao *et al.* firstly proposed a diffusion strategy to synthesize heteronetwork organohydrogels in 2017.<sup>44</sup> More specifically, an organohydrogel is formed by diffusing an oleophilic polymer dissolved in an amphiphilic solvent into a partially dehydrated hydrogel scaffold and then polymerizing it *in situ* to swell the organogel in the hydrogel, featuring interpenetrating oleophilic/hydrophilic heteronetworks. Secondly, emulsion polymerization is currently the most commonly used strategy for preparing heteronetwork organohydrogels that feature the binary cooperative phase, which can be applied to various hydrophilic and oleophilic monomers, and was proposed by Zhao *et al.* in 2017.<sup>47</sup> In this strategy, the hydrophilic and oleophilic monomer solutions are vigorously stirred or sonicated to form an oil-in-water emulsion. An emulsifier, including various surfactants or small-sized nanoparticles, should be added to the system to stabilize the emulsion resulting from the Pickering effect. The resulting emulsion shows that a large number of oil emulsion droplets with a diameter of several to tens of  $\mu\text{m}$  are uniformly distributed in the continuous water phase. Subsequently, heteronetwork organohydrogels in which micro-organogel domains are

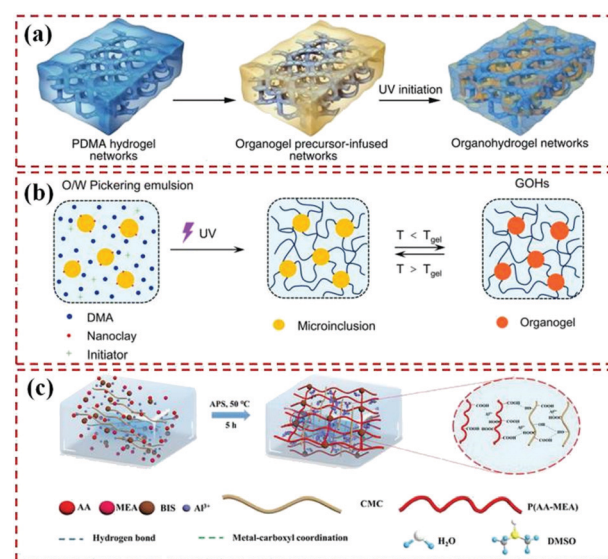


Fig. 2 Different preparation strategies of heteronetwork organohydrogels. (a) Preparation of an organohydrogel by diffusing the oleophilic polymer into a hydrogel scaffold to form interpenetrating structures. Reproduced under terms of the CC-BY license.<sup>44</sup> Copyright 2017, Springer Nature. (b) Emulsion polymerization. Reproduced with permission.<sup>82</sup> Copyright 2021, American Chemical Society. (c) One-step copolymerization of hydrophilic and hydrophobic monomers in a binary solvent. Reproduced with permission.<sup>67</sup> Copyright 2021, John Wiley and Sons.

uniformly distributed in a continuous hydrogel network can be obtained after polymerization.<sup>78–80</sup> Due to the thermoplasticity of the organogels, these organohydrogels show adjustable mechanical properties at different temperatures. Lastly, in some cases, heteronetwork organohydrogels can also be prepared through a one-step copolymerization method in which hydrophilic monomers and hydrophobic monomers are directly added to the binary solvent system and then copolymerized.<sup>45,67</sup>

Despite the proven effectiveness, these methods are limited by the complicated polymerization conditions. Given that, other effective preparation methods have also been explored and further developments are needed in the future. Representatively, Li *et al.* developed a simple “*in situ*” transformation strategy to prepare organohydrogels by simply soaking poly(pentafluorophenyl acrylate) (pPFPA) gel into the blend solution containing both hydrophilic and oleophilic alkylamines, so that these amines could react with pPFPA and then convert them into the corresponding acrylamide polymers based on the aminolysis of pPFPA.<sup>81</sup> Specifically, there are no strict requirements for the solvent in the ammonolysis process, only the selected amine should get dissolved in it and should not react. This strategy can not only efficiently synthesize heteronetwork organohydrogels with outstanding mechanical properties, but also solve the limitation of interfacial copolymerization caused by the immiscibility of water and oil in conventional synthesis methods.

As for homogeneous organohydrogels, there are mainly two methods that have been developed to construct a homogeneous network in a binary water/organic dispersion medium (Fig. 3). Firstly, a facile one-pot sol-gel synthesis method involving *in situ* gelation of polymers in a binary solvent is proposed.<sup>83</sup> In this strategy, all components including polymer monomers, initiators, and cross-linking agents are added to the binary solvent before polymerization takes place. The synthesis process is simple and has been widely used in the preparation of various organohydrogels.<sup>15,23,43,70,84</sup> However, the polymerization process is inevitably affected by the solvent environment, and the addition of organic agents may hinder the gelation

process. Specific synthesis conditions need to be considered when different monomers are polymerized, which leads to restrictions on the diversity of organohydrogels. Driven by this, Zhou *et al.* first proposed another strategy for preparing organohydrogels containing a binary-solvent system, which is called solvent replacement.<sup>85</sup> More precisely, a pre-prepared hydrogel is immersed in a mixture of organic agents and water, and the organohydrogels are synthesized by replacing part of the free water in the hydrogel with organic molecules owing to the osmotic pressure. The solvent replacement process is very free and does not require additional processing, and can reach equilibrium in a short time. Correspondingly, this strategy avoids the complicated designs of polymerization conditions, and thereby it can be used for various types of organohydrogels.<sup>74</sup> Specifically, the performance of the organohydrogels prepared by solvent replacement, such as frost resistance, long-term stability, and mechanical properties, can be easily adjusted by changing the immersion time, concentration, or the type of organic agent.<sup>4,86</sup> Based on these advantages, a large number of organohydrogels constructed by the solvent displacement have been reported in the past several years.<sup>55,63,66,87,88</sup>

To sum up, we systematically list the advantages and disadvantages of different preparation strategies for organohydrogels in Table 1. Unfortunately, the development of organohydrogels is still in its infancy. Not only do the types of organohydrogels need to be expanded, but it is also necessary to synthesize organohydrogels with different microstructures, such as thin films or fibers, which is conducive to their development in flexible integrated electronics. Driven by this, further development and exploration of more effective, low-cost, and simple preparation methods are still needed, such as three-dimensional (3D) printing technology.

## 2.2. Unique advantages

The manifested macroscopic performance is completely determined by the composition and structure of materials. Due to the combination of binary solvent or complementary phases, organohydrogels hybridized by hydrogels and organogels exhibit not only the unique performances derived from individual gel components but also some synergistic performances, such as anti-freezing and water retention ability, solvent resistance, and shape memory effect. This section describes in detail the generation mechanism, research progress, and application prospects of these unique properties in organohydrogels.

**2.2.1. Anti-freezing and water retention ability.** In hydrogels, high water content is essential for maintaining ionic conductivity and structural integrity. However, water will inevitably transform into the ice phase at freezing temperatures, which causes the hydrogel to become rigid, brittle, opaque, and lose its functionality. In general, the optimal design of the composition and molecular structure of a hydrogel is the key point to improving its frost resistance. The inhibition of ice nucleation and ice-crystal growth at lower temperatures is very important for the development of hydrogel-based devices that work normally at low temperatures. Inspired from natural phenomena, where remarkable freezing tolerance in plants and animals is introduced by the



Fig. 3 Typical fabrication strategies of homogeneous organohydrogels. (a) A one-pot sol-gel synthesis method. Reproduced with permission.<sup>84</sup> Copyright 2017, John Wiley and Sons. (b) The solvent replacement strategy. Reproduced with permission.<sup>63</sup> Copyright 2019, Royal Society of Chemistry.

Table 1 Comparison of the advantages and disadvantages of various methods for preparing organohydrogels

Types	Methods	Advantages	Disadvantages
Heteronetwork organohydrogel	<i>In situ</i> polymerization of oleophilic polymer diffused into the hydrogel scaffold	Less restricted by polymerization conditions due to separate polymerization process The resulting organohydrogels both combine the characteristics of hydrophilic and oleophilic polymers and exhibit adaptive surface wettability	More preparation steps The hydrophilic and oleophilic network may not fully interpenetrate due to the intrinsic incompatibility of water and oil phase, resulting in undesirable functionality Interfacial copolymerization is suppressed to a certain extent
	Emulsion polymerization	Resulting in the effective combination of hydrogel and organogel at micro/nanoscale dimensions Enabling the organohydrogels to display adjustable mechanical properties	The use of large amounts of emulsifiers may increase the toxicity of the system Interfacial copolymerization is restricted
	One-step copolymerization of hydrophilic and hydrophobic monomers in binary solvent	Simple and fast	The polymerization of different polymers under the same conditions is limited, resulting in poor diversity of organohydrogels
Homogeneous organohydrogel method	One-pot sol-gel synthesis	Fast and straightforward	Changes in the polymerization conditions of the polymer limit the successful preparation of various organohydrogels after the introduction of organic solvents
	Solvent replacement strategy	No restrictions on the polymerization conditions Various properties of the final organohydrogels can be easily controlled by the immersion time, concentration or the type of organic agents	More steps than one-pot method The conductivity may be decreased

increased quantities of fatty species in biological organisms, fascinating frost resistance is demonstrated in organohydrogels by the introduction of organic solvents. Among the reported organic solvents for organohydrogels, EG is the simplest and cheapest, and the freezing point of the water/EG binary solution can be decreased to below  $-40\text{ }^{\circ}\text{C}$ .<sup>89</sup> To this end, a PVA/poly(3,4-ethylenedioxythiophene):polystyrene sulfonate (PEDOT:PSS) organohydrogel was reported by using the water/EG binary solvent, which exhibited stable flexibility and strain-sensitivity in the temperature range from  $-55.0$  to  $44.6\text{ }^{\circ}\text{C}$ .<sup>49</sup> Gly is also a well-known, nontoxic anti-freezing agent, and is most commonly

used in the preparation of organohydrogel because of its good biocompatibility and better freezing resistance.<sup>90,91</sup> For instance, Sun *et al.* proposed an anti-freezing polyacrylamide (PAM)/montmorillonite/carbon nanotube (CNT) organohydrogel based on a water/Gly binary solvent system, and it can maintain mechanical flexibility and good conductivity over a broad temperature range ( $-60$  to  $60\text{ }^{\circ}\text{C}$ ) (Fig. 4a-c).<sup>66</sup> Similarly, the gelatin supramolecular organohydrogel could retain 100% stretchability even at  $-70\text{ }^{\circ}\text{C}$ , owing to the use of a water/Gly binary solvent.<sup>55</sup>

In particular, DMSO is a very common cryoprotectant and has been widely applied for cryopreserving cells.<sup>92,93</sup> A water/DMSO binary solvent has also been used for fabricating organohydrogels, and their freezing points are effectively reduced.<sup>94</sup> Ye *et al.* reported a cellulose nanofibril (CNF) based organohydrogel by using the water/DMSO binary solvent, which could remain flexible and well conductive at  $-70\text{ }^{\circ}\text{C}$ .<sup>95</sup> In detail, the freezing point may reach the lowest temperature of  $-115\text{ }^{\circ}\text{C}$  by adjusting the ratio of DMSO/water to a 7:3 molar ratio. In addition to these, the introduction of other organic agents can also lead to good frost resistance in organohydrogels. Chen *et al.* reported the utilization of sorbitol to fabricate Ca-alginate/PAM organohydrogels with good mechanical flexibility at  $-45\text{ }^{\circ}\text{C}$ .<sup>85</sup> Gao *et al.* exploited water and heptanes as the dispersion medium of the hydrophilic/oleophilic heteronetwork organohydrogel, the organohydrogel showed reversible and stable elasticity even at a temperature as low as  $-78\text{ }^{\circ}\text{C}$ .<sup>44</sup> In general, the proportion of binary solvent is vital for the anti-freezing properties of organohydrogels. Previous studies have shown that the freezing point reaches the lowest when the weight percent of Eg and Gly is 70 and 66%, respectively.<sup>4,43,84</sup>

In these cases, the ice inhibition effects in organohydrogels strongly put down to the formation of strong hydrogen bonds between the organic agents and the water molecules. There are



Fig. 4 The frost resistance performances and mechanism of organohydrogels. (a) Photographs showing the flexibility; (b) stress-strain curves; and (c) conductivity of MMCH (hydrogel) and MMCOH (organohydrogel) at various temperatures. Organohydrogels maintain excellent mechanical properties and conductivity at sub-zero temperatures, showing an outstanding anti-freezing ability. Reproduced with permission.<sup>66</sup> Copyright 2021, John Wiley and Sons. (d) Schematics illustrating the anti-freezing mechanism of organohydrogels. Reproduced with permission.<sup>67</sup> Copyright 2021, John Wiley and Sons.

three different states of water in hydrogels: free water, intermediate water, and strongly bound water.<sup>96</sup> The free water can easily freeze at normal freezing points and exchange rapidly with different organic solvents. The intermediate water is weakly bound with polymer chains or other chemicals in the hydrogels, which can freeze at lower temperatures. In particular, the strongly bound water can keep it from freezing even when the temperature is below  $-100\text{ }^{\circ}\text{C}$ , owing to the formation of more than one hydrogen bond with the polymer and others. In general, water crystallization is the formation of an infinite hydrogen bond network of water molecules.<sup>97</sup> The organic solvent in organohydrogels can partially replace free water and form hydrogen bonds with the surrounding water molecules, which is beneficial to reduce the fraction of free water and meanwhile disrupts the hydrogen bonds between water molecules, thereby enhancing frost resistance (Fig. 4d).<sup>87</sup> Thus, compared with EG-based organohydrogels, the better freezing resistance in Gly-based organohydrogels can be attributed to the three hydroxyl groups in Gly that can form bonds with the surrounding water molecules.

In addition to water crystallization, water evaporation can also cause detrimental effects on the properties of the hydrogels, including the weakening of mechanical properties and ionic conductivity, shape deformation, or generation of cracks. The excellent water retention ability of hydrogels is necessary to achieve long-term stability even under arid conditions. In previous studies, the simplest and most common strategy to reduce water evaporation is to encapsulate hydrogels with elastomers.<sup>98</sup> However, the encapsulation will cause a sophisticated fabrication process or even a dragged down mechanical performance, and the loss of water cannot be completely avoided. Attractively, an excellent drying tolerance can be achieved in organohydrogels. Wu *et al.* reported a MXene nanocomposite organohydrogel with the water/Gly binary solvent as the dispersion medium, thus leading to the long-lasting moisture retention of these organohydrogels (10 days) (Fig. 5a and b).<sup>70</sup> Lu *et al.* prepared a conductive organohydrogel by using the water/Gly binary solvent, and there was no performance degradation even after a long period of storage (30 days) (Fig. 5c–g).<sup>84</sup> Consequently, the construction of organohydrogel seems to be a more effective method to inhibit water evaporation without losing mechanical properties.

In general, the evaporation of water is caused by the lower vapor pressure of the surrounding environment than that of the hydrogels. Organic agents generally have a higher boiling point and can reduce the vapor pressure after mixing with water. Typically, Gly is a well-known, nontoxic humectant with excellent hygroscopicity. Compared with similar hygroscopic EG, Gly has a better water retention ability due to its higher viscosity, higher boiling point, and lower vapor pressure.<sup>63</sup> Consequently, the outstanding water retention ability in the organohydrogels can be attributed to the closer vapor pressure between the materials and surroundings. Additionally, the interaction between organic molecules and the network also plays an important role in inhibiting water evaporation such as the ample and strong hydrogen bonds formed with water molecules.<sup>43</sup> Considering the relatively high dissociation energy of these bonds, they can even exist stably at a higher temperature, resulting in a lower



Fig. 5 The water retention ability of organohydrogels. Comparison of flexibility between a MXene nanocomposite organohydrogel and a hydrogel through (a) twisting and (b) bending after storage for 10 days. Reproduced with permission.<sup>70</sup> Copyright 2020, Royal Society of Chemistry. (c) Photographs of the GW-hydrogel (organohydrogels) and the W-hydrogel (hydrogels) after being placed in air for 30 days or after 1 day of freeze drying; (d) The change curve of the weight of the GW-hydrogel and the W-hydrogel with storage time; Comparison of (e) compression strength, (f) tensile strength and (g) maximum tensile strain of the GW-hydrogel and the W-hydrogel in the initial state or after storage for 30 days at 25 and  $-20\text{ }^{\circ}\text{C}$  or after freeze-drying, reflecting the excellent stability of organohydrogels. Reproduced with permission.<sup>84</sup> Copyright 2017, John Wiley and Sons.

drying speed and increased environmental tolerance of the resulting organohydrogels.

The representative developments of the anti-freezing and water retention capabilities of organohydrogels are summarized in Table 2, and obviously their working temperature range and service life are effectively extended. Generally, at a sub-zero temperature, in addition to inhibiting the freezing of water molecules in the bulk phase, the freezing of water molecules adsorbed on the surface of the organohydrogels also needs to be prevented. However, the latter is rarely involved. Additionally, although the loss of water is greatly alleviated in the organohydrogel, dehydration will inevitably occur under extremely arid environments or after long-term use. Ideally, we urgently hope to develop a self-regeneration organohydrogel, which can self-regenerate to its original state for reuse. Recently, a LiCl-based hydrogel with strong water retention and self-regeneration abilities was reported. After vacuum drying, the dehydrated hydrogel could recover to its original state by spontaneously absorbing water molecules from the surrounding environments because of its lower vapor pressure.<sup>68</sup> As water absorption from moisture has also been discovered in organohydrogels,<sup>64,85</sup> we believe that self-regeneration of organohydrogels can also be achieved by regulating the proportion of organic agents and the humidity of the storage

Table 2 The development of anti-freezing and water retention capabilities of representative organohydrogels

Organohydrogel	Solvent composition	Preparation method	Freezing resistance	Dry resistance	Published year
PVA/PEDOT:PSS organohydrogel <sup>49</sup>	Water/EG	One-pot sol-gel synthesis method	-55 °C	—	2017
Hydrophilic/oleophilic hetero-network organohydrogel <sup>44</sup>	Water/ <i>n</i> -decane Water/heptanes	Diffusion strategy	-15 °C -78 °C	—	2017
PDA-CNTs/PAM/PAA organohydrogel <sup>84</sup>	Water/Gly	One-step copolymerization	-20 °C	90% weight retention after 7 days (60 °C)	2018
Ca-Alginate/PAM organohydrogel <sup>85</sup>	Water/Gly Water/EG Water/sorbitol	Solvent displacement	-50 °C -70 °C -45 °C	88%, 45%, 75% weight retention after freeze-drying	2018
Gelatin supramolecular organohydrogel <sup>55</sup>	Citrate (Cit)/ water/Gly	Solvent displacement	-80 °C	90% weight retention after 7 days (20 °C, 50% RH)	2019
PVA/CNF organohydrogel <sup>95</sup>	Water/DMSO	One-pot sol-gel synthesis method	-70 °C	60% weight retention after 24 h (40 °C, 15% RH)	2020
TA@CNF/MXene/PAM organohydrogel <sup>23</sup>	Water/Gly	One-step copolymerization	-80 °C	80% weight retention after 7 days (20 °C, 35% RH)	2020
Alginate/(poly(ethylene glycol) diacrylate (PEGDA) organohydrogel fibers <sup>74</sup>	Water/Gly/CaCl <sub>2</sub> / KCl	Solvent displacement	-100 °C	90% weight retention after 10 days (20 °C, 45% RH)	2020
PAM/montmorillonite/CNT organohydrogel <sup>66</sup>	Water/Gly	Solvent displacement	-60 °C	90% weight retention after 3 days (25 °C) 77.5% weight retention after 72 h (60 °C)	2021
Carboxymethyl cellulose sodium salt (CMC)/P(AA-MEA) organohydrogel <sup>67</sup>	Water/DMSO	One-step copolymerization	-90 °C	76% weight retention after 15 days (normal temperature)	2021

environment. Moreover, there are other feasible methods to fabricate anti-freezing and anti-drying hydrogels, such as the incorporation of inorganic salts (*e.g.* NaCl, CaCl<sub>2</sub>, and ZnCl<sub>2</sub>) and zwitterionic osmolytes (*e.g.* betaine or proline), which can also be used synergistically to further broaden the working environment of organohydrogels.<sup>4,23,68</sup>

**2.2.2. Solvent resistance.** Recently, flexible electronic devices that can operate in complex liquid environments have received copious attention. Conventional hydrogels can easily swell or shrink in their respective good or poor solvents. The deformation of the hydrogels will be detrimental to their various performance and functionalities, such as mechanical strength, toughness, self-adhesion, or conductivity.<sup>45,99</sup> Therefore, solvent resistance is a necessary requirement for the future development of devices that can work normally in water or organic solvents. Interestingly, heteronetwork organohydrogels formed by mixing hydrophilic/oleophilic networks in a multi-solvent system can well solve this common problem. The combination of these binary components with entirely opposite physicochemical properties can compensate for the deficiency of a homogeneous single network. When equilibrated in a certain solvent, the swollen polymer network is always constrained by the other shrunken polymer network, resulting in no obvious volume change being found.<sup>44</sup> Although excellent solvent resistance is achieved, the diffusion of free ions into the solvent in an ion-conductive organohydrogel can lead to instability of conductance due to osmotic pressure. Correspondingly, the electronic conduction system provides great possibilities for electronic devices that can work stably in various solvents. Hence, Liu *et al.* prepared a graphene-assisted conductive organohydrogel by copolymerization of a hydrophobic monomer (2-methoxyethyl acrylate (MEA)) and a hydrophilic monomer (acrylic acid (AA)) in a

mixed solvent of water and DMSO,<sup>45</sup> and the resulting synergistic hydrophobic and hydrophilic network system endowed the organohydrogel with excellent solvent resistance (Fig. 6a-d). Significantly, this organohydrogel could serve as an all-weather wearable sensor and even achieve accurate and stable mechanical sensing in diverse solvents.

In particular, owing to the intrinsic immiscibility and the opposite solvent affinities of the hydrophilic and hydrophobic networks, the heteronetwork organohydrogels can controllably and reversibly rearrange their surface structure according to the different surrounding media, and realize adaptive superhydrophilic and superoleophilic transitions.<sup>46</sup> In this case, the organohydrogel exhibits amphiphilic surface properties in dry air. When the organohydrogel is immersed in water, the hydrophilic network can absorb water and swell while the hydrophobic network is squeezed inward, resulting in a hydrogel-dominated surface reconfiguration and subsequent superhydrophilic surface properties. In contrast, organohydrogels exhibit superoleophilic surface properties in oil due to the occurrence of organogel-dominated surface reconfiguration (Fig. 6e). To this end, an organohydrogel with adaptive macroscopic wetting properties was synthesized by polymerizing an oleophilic monomer (lauryl methacrylate and *n*-butyl methacrylate) in a three-dimensional crosslinked hydrophilic matrix, which has potential application in smart gating systems, such as on-demand oil/water separation.<sup>44</sup>

Furthermore, by taking advantage of the hydrophilic/hydrophobic interactions that exist simultaneously in the system, Wan *et al.* reported a surface patterning technique that uses pre-patterned substrates with different wettability regions to induce patterning of hydrophilic and hydrophobic monomers at the solid-liquid interface through hydrophilic/hydrophobic



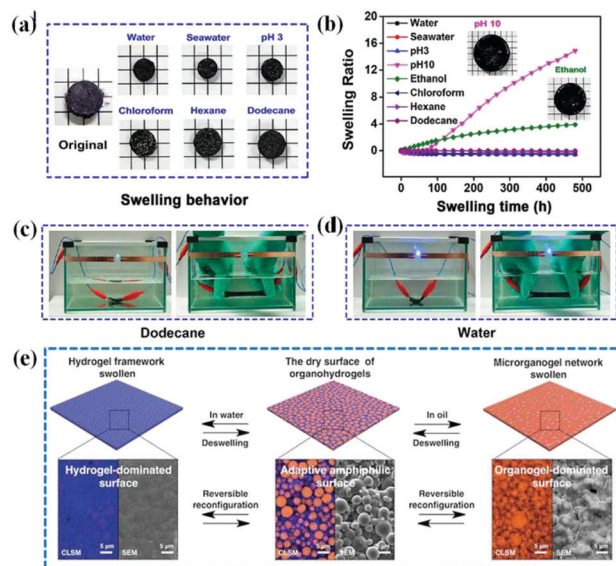


Fig. 6 The anti-swelling and adaptive wettability of heteronetwork organohydrogels. (a) Photographs of the swelling behavior of organohydrogels after swelling 20 days in various solvents and the corresponding (b) swelling ratio change of organohydrogels as a function of swelling time; stable conductivity of organohydrogels in (c) dodecane and (d) water for strain sensing in various liquid media. Reproduced with permission.<sup>45</sup> Copyright 2020, American Chemical Society. (e) Schematic diagram of reversible switching between the hydrogel- and organogel-dominated surface states of the organohydrogel as the solvent changes. Reproduced with permission.<sup>46</sup> Copyright 2019, John Wiley and Sons.

interactions, and then *in situ* polymerization to fix the patterns on the organohydrogel surface.<sup>65</sup> The surface-patterned organohydrogels can be well maintained in diverse solvents, owing to their excellent solvent resistance. Additionally, focusing on the obvious transparent change of the heteronetwork organohydrogel resulting from the microphase separation in poor solvents and low-swelling in suitable solvents, Liu *et al.* proposed a dynamic information memory device for recording and encrypting information based on the variable and adjustable optical properties.<sup>67</sup> Similarly, this organohydrogel still exhibits anti-swelling properties owing to the introduction of the hydrophobic and hydrophilic components. Therefore, in combination with such commendable solvent resistance, heterogeneous organohydrogels not only exhibit an excellent environmental tolerance but also can work normally in a variety of water or oil-based liquid phase environments like water, n-dodecane, chloroform, and hexane; hence, they have shown great potential for applications in various fields such as underwater robots, underwater sensing, implantable bioelectronics, and oil-water separation.

**2.2.3. Shape memory effect.** In addition to the above-mentioned excellent properties, the heteronetwork organohydrogel prepared by emulsion polymerization also exhibits a shape memory effect. This refers to a phenomenon in which materials can fix temporary shapes and return to their original shapes under external stimuli (*e.g.*, pH, heat, light, chemicals, electrical stimulation, magnetic stimulation),<sup>100–103</sup> and these smart materials with the shape memory effect have a wide range of

potential application in electronics, aerospace, biomedical, and tissue engineering settings.<sup>104–110</sup> The composition design of shape memory materials should meet two basic requirements at the same time. The first is that the materials need to hold stable netpoints to maintain the permanent shape, and the other is that they need to contain stimuli-switchable units to fix the temporary shape.<sup>111</sup> Among the typical shape memory materials reported, solid shape memory polymers (SMPs) based on glass or melting-crystallization transitions have a high density of netpoints and low polymer-chain mobility, and thus suffer from limited strain capacity. Even the highly stretchable SMPs cannot fully recover from strains over 1000%,<sup>47,112,113</sup> which severely limits their practical applications. By contrast, shape memory hydrogels (SMHs) can significantly improve the strain capacity due to their excellent stretchability, but the elastic modulus is decreased.<sup>100</sup> Furthermore, the shape memory effect of most SMHs mainly relies on the reversible supramolecular interactions or dynamic covalent/non-covalent bonds as molecular switches, so it is difficult to achieve the fixation and recovery of elastic deformation.<sup>114–116</sup>

Given these limitations, a high-strain and tough shape memory organohydrogel with a binary cooperative phase was prepared, and its shape memory effect was closely related to the phase transition of the paraffin composition in the micro-organogel domains by thermal stimuli.<sup>47</sup> As illustrated in Fig. 7a and b, at room temperature, this organohydrogel exhibited excellent strength and toughness due to the reinforcement of micro-organogel domains, and the micro-organogel domains exist in spherical shapes to maintain the lowest energy of the system. When the organohydrogel is heated above the melting point ( $T_m$ ) of paraffin, the micro-organogel domains will soften accordingly. Meanwhile, the sample can be more easily stretched into a specific shape, and the micro-organogel domains change from spherical to ellipsoidal shapes along the stretching direction. By reducing the temperature from over  $T_m$  to below  $T_m$ , the correspondingly frozen paraffin will keep the micro-organogel domains in the deformed shape and prevent the elastic deformation of the hydrogel network through covalent interconnection at the heterophase interfaces, resulting in a fixed temporary shape of the organohydrogel at the macro-scale and the energy storage in the system. When the temperature increases above  $T_m$  again, the elastic potential energy in the hydrogel network and the interfacial tension of the micro-organogel domains drive the organohydrogel to release energy so as to completely return to its original shape with the lowest energy. In this case, the organohydrogel is accompanied by energy storage and release during the shape memory process, which is conducive to the recovery of elastic deformation.

According to this mechanism, it is anticipated that multiple shape memory effects can be achieved by combining multiple noneutectic phase transition components inside microorganogel inclusions. Subsequently, Zhuo *et al.* prepared a complex multiphase organohydrogel by incorporating microorganogel inclusions containing multiple oleophilic components with different phase transition temperatures in continuous elastic

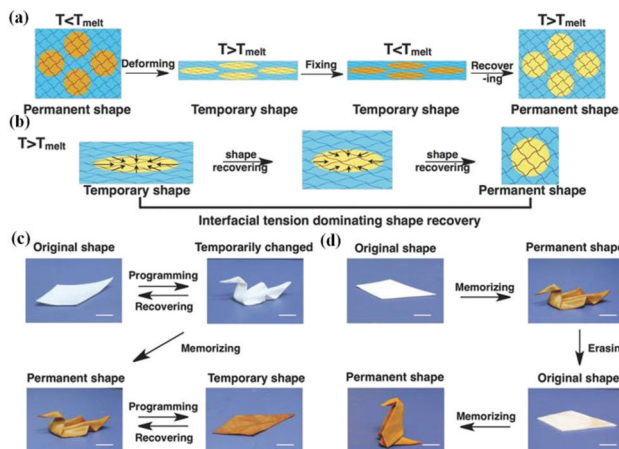


Fig. 7 Shape memory effect of the heteronetwork organohydrogels. (a and b) Schematic illustration of the shape memory process of the organohydrogel based on the phase-transition of micro-organogels. Reproduced with permission.<sup>47</sup> Copyright 2017, John Wiley and Sons. (c and d) Hierarchical shape morphing process. Reproduced with permission.<sup>117</sup> Copyright 2018, John Wiley and Sons.

hydrogel networks.<sup>80</sup> For example, assembling  $C_{16}H_{34}$  and  $C_{28}H_{58}$  with significantly different alkyl chain lengths and poly(stearyl methacrylate) (PSMA) within the microorganogel inclusions provided the organohydrogel with precisely controllable thermo-induced triple-switching mechanical properties due to the triple-phase transitions of the microorganogel inclusions from a fully crystalline state to a fully melting state as the temperature varies.

Considering the dual-phase heteronetworks in an organohydrogel, Zhao *et al.* developed a dual-programmable shape-morphing organohydrogel containing micro-organogel inclusions and the reversible metallo-supramolecular hydrogel framework, which can independently respond to different stimuli.<sup>117</sup> On the one hand, the reversible metal–ligand association/dissociation of the hydrogel framework realizes the permanent shape memorization process *via* depressing the storage energy of the previous temporary state. On the other hand, the micro-organogel inclusions with thermoswitchable phase-transition ability dominate the shape memory process. This hierarchical shape morphing behavior enables versatile step-wise memorization and programming of geometrically complex structures (Fig. 7c and d). Specifically, note that this adaptive smart organohydrogel could adjust the surface topographies and properties simultaneously, a smart microfluidic device was developed accordingly to enable on-demand remote programming of unidirectional liquid transport by the integration of photothermal  $Fe_3O_4$  nanoparticles.<sup>46</sup> Nevertheless, although the huge application potential of these smart organohydrogels has been proven, it is still a long way from the laboratory to practical applications.

### 3. Optimal design of organohydrogels

In addition to these inherent excellent properties derived from the unique components and structure of organohydrogels, there are still some other properties that need to be included

or further optimized through additional means to meet the practical applications of organohydrogels in various fields, such as mechanical properties, conductivity, self-healing, adhesion, antibacterial properties, *etc.* Herein, this section summarizes the reported optimization strategies for the various properties of organohydrogels in detail.

#### 3.1. Mechanical properties

Flexible electronic devices usually need to exhibit good mechanical properties, including strong strength, high stretchability, and good fatigue resistance, and this is mainly determined by the cross-linking method and degree between various components of the gel network.<sup>5</sup> In general, chemical cross-linking is mainly based on strong covalent bonds, which can significantly improve the mechanical strength, but the breaking of these covalent chemical bonds under large deformation will cause irreversible damage to the structure, thus leading to poor deformation tolerance and fatigue resistance.<sup>2,87</sup> Conversely, a purely physical cross-linking network based on the reversible non-covalent interactions, such as hydrogen bonds,  $\pi$ -stacking interactions, and van der Waals interactions, can easily recover and rebuild under deformation.<sup>35</sup> As for traditional hydrogels, they generally exhibit low mechanical strength due to high water content and loose cross-linking, and are prone to breakage during mechanical deformations, which is not conducive to practical applications.<sup>1</sup> To solve this problem, multiple reversible non-covalent interactions are introduced into the strong chemical cross-linking network, which can dissipate energy as sacrificial bonds during the stretching process and reassociate after the stress is removed, making the hydrogel exhibit both good mechanical strength and high toughness.<sup>4,55</sup>

Organohydrogels generally exhibit better mechanical properties than hydrogels composed of the same polymer network due to the following two points. First of all, the organic agents in the organohydrogels will form a large number of hydrogen bonds with water and polymers in the network, which can increase the cross-linking density of the polymer network and facilitate the bridging of polymer chains,<sup>84,85,87</sup> resulting in enhanced mechanical properties. For instance, Fang *et al.* prepared a gelatin/ferric-ion-cross-linked polyacrylic acid (PAA) dual dynamic supramolecular network, which can be toughened by incorporating Gly into the gel networks because of the significantly increased physical cross-linking of gelatin and reduced phase separation.<sup>88</sup> However, when the organic solvent is excessive, it will cause rapidly increased cross-link density of hydrogen bonds and even volume shrinkage, which is not conducive to the movement of polymer molecular chains, making the resulting organohydrogels extremely fragile.<sup>85</sup> In general, the mechanical performance of the organohydrogels largely depends on the proportion of organic solvent in the mixture.

Secondly, organohydrogels exhibit enhanced mechanical strength without sacrificing much flexibility because the organic agents in them can induce polymer crystallization.<sup>49,95</sup> For instance, different from other conventional PVA hydrogels with low mechanical strength, high-strength organohydrogels combined with the water/EG binary solvent were reported. This strength enhancement is mainly derived from the crystallization of PVA after the introduction of EG, and the strength continues

to increase with the increasing EG concentration due to the formation of more induced PVA crystalline domains.<sup>49</sup> Furthermore, a highly stretchable, strong, and tough PVA-based organohydrogel was also fabricated by using the water/DMSO binary solvent; the excellent mechanical strength was also ascribed to the crystallization of PVA chains, which was formed because of the strong intermolecular interaction between DMSO and water and thus the insufficient solvation of PVA chains.<sup>95</sup> In these cases, the formed crystalline domains not only served as rigid and high-functionality crosslinkers to strengthen the network, but also toughened the organohydrogels through the crack pinning effect,<sup>18,49</sup> thereby providing better mechanical properties compared to hydrogels.

In fact, it is necessary to further improve the mechanical properties of existing organohydrogels. In a single polymer network, the low density or irregular distribution of cross-linking points results in different polymer chain lengths, and this intrinsic structural inhomogeneity easily causes initial cracks. Moreover, organohydrogels are prone to rupture due to the lack of sufficient energy dissipation mechanism to slow down the propagation of cracks. To address this problem, tremendous improvements have been made to fabricate strong and tough organohydrogels by introducing energy dissipation mechanisms, such as forming a double network (DN),<sup>43,63,87,118</sup> adding nanofillers,<sup>16,84,95,119</sup> introducing other dynamic interactions,<sup>86,120,121</sup> and creating nano-crystalline domains.<sup>88</sup>

Above all, the incorporation of a second polymer network is an effective strategy to strengthen and toughen organohydrogels and keep other functions from being lost.<sup>122,123</sup> Generally, the obtained DN hydrogel is composed of two complementary polymer networks with different physical natures, either physically (PVA,<sup>43</sup> agar,<sup>123</sup> alginate,<sup>122</sup> carrageenan,<sup>124</sup> gelatin<sup>88</sup>) or chemically cross-linked (PAM,<sup>43,70,87</sup> PAA<sup>43,64</sup>). During the stretching process of the materials, the physically crosslinked polymer network is broken first to dissociate and dissipate energy, resulting in an increase in toughness. Meanwhile, the chemically cross-linked network remains intact and stabilizes the deformation to provide the materials with good mechanical strength. In addition, the interactions between these two polymer networks also dissipate mechanical energy so as to continue to improve the mechanical properties of the materials. As a consequence, this incorporation ultimately results in the combination of relatively high stiffness and high toughness of the material, which has important advantages over traditional single-network organohydrogels with weak and brittle nature.

Secondly, adding nanofillers to the polymer network can also effectively reinforce the organohydrogels, which have been widely used in previous studies. So far, many nano-filled materials have been reported to be incorporated into organohydrogels, such as CNTs,<sup>16,66,84</sup> silk nanofibers (SNFs),<sup>119</sup> CNFs,<sup>23,95</sup> graphitic carbon nitride ( $g\text{-C}_3\text{N}_4$ ),<sup>119</sup> and silica nanoparticles.<sup>73</sup> It is worth noting that the mechanical properties of the composite organohydrogels are largely determined by the chemical nature and dispersivity of the fillers.<sup>125,126</sup> The weak interfacial interactions between the filler and the polymer matrix are not conducive to an effective load transfer between

them.<sup>127,128</sup> In order to effectively improve the mechanical properties of the organohydrogel, the filler added generally has a large number of functional groups, and the reinforcing effect can be attributed to the formation of dynamic hydrogen bonds.<sup>129</sup> Very recently, Bao *et al.* reported the utilization of soft SNFs and hard  $g\text{-C}_3\text{N}_4$  nanosheets to co-reinforce a PVA organohydrogel.<sup>119</sup> The functional groups on the surface of  $g\text{-C}_3\text{N}_4$  nanosheets and the molecular chain of silk nanofibers, such as amide groups, carboxyl groups, and amino groups, could form reversible hydrogen bonds with the PVA molecular chains, and thus greatly improve the tensile strength and toughness of the organohydrogel (Fig. 8a and b). Driven by this, the chemical nature of the fillers can be effectively changed by modifying the functional groups to strengthen interfacial interactions with polymer networks, which is an effective approach for hydrogel reinforcement.<sup>130</sup> For example, Jaiswal *et al.* proposed a mechanically stiff nanocomposite hydrogel by incorporating nanoparticles functionalized with nitro-dopamine anchored PEG diacid on the surface, which resulted in a more than 10-fold increase in mechanical stiffness and a 20-fold increase in toughness due to the enhanced nanoparticle-polymer interactions.<sup>131</sup>

In this strategy, it cannot be ignored that these fillers, especially for CNTs, are prone to aggregation in the gel due to their inherent surface hydrophobicity and strong van der Waals force, which in turn lead to a decrease in the mechanical properties of the organohydrogels due to the uneven distribution of the structure. According to previous reports, this can be properly resolved by adding stabilizers or dispersants to the

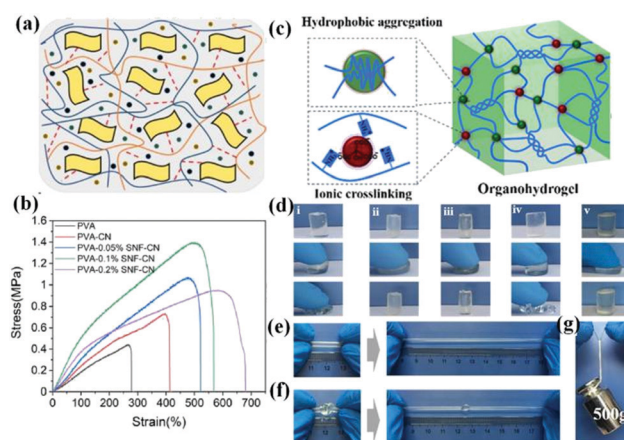


**Fig. 8** Structural design and mechanical performance characterization of tough organohydrogels. (a) Schematic diagram of SNF and  $g\text{-C}_3\text{N}_4$  nanosheet incorporated organohydrogel. (b) Comparison of the stress-strain curves between a nanocomposite organohydrogel and a pure organohydrogel. Reproduced with permission.<sup>119</sup> Copyright 2021, Elsevier. (c) Schematic diagram of a supramolecular organohydrogel prepared in a citrate water/glycerol mixture solution. (d) Compression performances of various gelatin gels (i) hydrogel, (ii) supramolecular hydrogel 1, (iii) supramolecular organohydrogel, (iv) organohydrogel, and (v) supramolecular hydrogel 2), showing the improvement in the mechanical properties by supramolecular interaction; mechanical performance of a supramolecular organohydrogel under (e) stretching, (f) knotting and (g) 500 g load. Reproduced with permission.<sup>55</sup> Copyright 2019, American Chemical Society.

aqueous solution of CNTs, such as polydopamine (PDA),<sup>84</sup> tannic acid (TA),<sup>16</sup> and montmorillonite (MMT).<sup>66,126</sup> The good dispersibility achieved is caused by the repulsion between the functional groups of the agents attached to CNTs or between dispersants and CNTs. In particular, the mechanical properties of these organohydrogels can be further improved due to the increased interaction between dispersants and the polymer network.

Thirdly, the addition of ions enables the strengthening of the organohydrogel by forming ionic interactions with polymer chains and thereby increasing the cross-linking density.<sup>55,67,121,132</sup> Particularly, apart from the formed coordination bonds, the introduced ions can also adjust the mechanical properties by influencing the aggregation/crystallization of polymer chains, that is, the Hofmeister effect or ion-specific effect.<sup>18</sup> Generally, some ions can combine with the surrounding hydration water molecules of the polymer chains and make them polarized, resulting in the instability of the hydrogen bonds between the polymer chains and their hydration water molecules, and finally the water molecules can be discharged from between the polymer chains (salting-out effect). Meanwhile, the polymer chains aggregate through the formation of hydrogen bonds between the hydrophilic groups of the polymer chains, exhibiting a strong reinforcement effect.<sup>133</sup> For example, a tough gelatin supra-molecular organohydrogel was prepared by immersing the pre-hydrogel in concentrated sodium citrate water/Gly solution.<sup>55</sup> Its excellent flexibility and mechanical strength can be attributed to the formation of multiple non-covalent supra-molecular cross-linking, such as the hydrophobic aggregation induced by the salting-out effect, ionic interactions between the  $-\text{NH}_3^+$  of gelatin and  $\text{Cit}^{3-}$  anions, and quadruple hydrogen bonding (Fig. 8c–g). Specifically, studies have shown that when ions are introduced, the improvement of mechanical properties caused by the formation of induced crystalline domains is more effective than the traditional strengthening achieved by ionic cross-linking.<sup>134,135</sup> Additionally, some ions can directly bond with the polymer chain and dissociate the hydrogen bonds between the polymer chains, leading to the increase of polymer solubility and the softening of the network (salting-in effect). For instance,  $\text{Fe}(\text{NO}_3)_3$  was found to have a strong salting-in effect on PVA hydrogels, which can make the tough hydrogels soften quickly. Inspired by this, a hydrogel that can switch *in situ* between the stiff and soft states was proposed, which hopefully can be used as a neuron probe.<sup>133</sup> However, organohydrogels with adjustable mechanical properties have not yet been involved, which is quite necessary for their future developments.

Even so, these methods mentioned above mainly focus on composition or molecular engineering, which rarely involve structural changes. In a single and homogeneous covalent polymer network, high crack resistance and high elastic modulus cannot be realized simultaneously.<sup>136</sup> In contrast to homogeneous tough polymer networks made by molecular engineering methods, creating anisotropic micro/nanostructures in hydrogel can well resist the growth of a crack, achieving both high toughness and fatigue resistance. General structural engineering methods include ice-templating,<sup>137</sup> mechanical stretching,<sup>138,139</sup>

and compositing.<sup>136,140</sup> The ice-templating method can lead to the formation of micro-alignment structures in the material. And mechanical stretching can also effectively create anisotropic micro/nanostructures. The formation of these micro/nanostructures in a hydrogel will lead to an increase in material density to strengthen the material, and the increased toughness is attributed to the increased energy dissipation during fracture. The most common strategy for compositing methods is to add alien micro/nanoscale fibre reinforcements to the hydrogel. To better improve the fatigue resistance of materials, this compositing method needs to follow the principles that the fibre reinforcements should be stiffer than the matrix and the interface adhesion should be strong.<sup>136</sup> The soft matrix facilitates the stress transfer in the network. Ideally, the initial crack will not cause serious stress concentration in the fibers but spreads to the entire network, and the crack propagation is also prohibited by the fibers, showing a crack-blunting ability (Fig. 9a). Consequently, this composite hydrogel requires more energy to grow the crack and shows a gradual failure mode featuring stepwise fracture and pull-out of fibres.<sup>141–143</sup> Based on this, Ge *et al.* developed a highly stretchable PAA organohydrogel by incorporating polyaniline nanofibers (PANI NFs) into the network, taking advantage of the fiber-reinforced microstructures.<sup>132</sup>

At present, the effective combination of molecular and structural engineering strategies is an important way to construct gel materials with better mechanical properties.<sup>144</sup> Recently, Hua *et al.* presented a freezing-assisted salting-out treatment to produce a hierarchically anisotropic hydrogel, which in turn formed a mesh-like stretchable nanofibril network on the surface of the micrometre-scale aligned pore walls, showing a high toughness value that even surpass natural tendons and spider webs.<sup>18</sup> Concretely, directional freeze-casting causes the hydrogel to form aligned micropore walls and correspondingly leads to an increase in material density. The subsequent salting out strongly



Fig. 9 Structural engineering in organohydrogels. (a) Toughening mechanisms at each length scale. Reproduced with permission.<sup>18</sup> Copyright 2021, Springer Nature. Schematic design of (b) PVA hydrogels with a microfibrillar network and (c) PVA organohydrogels with a nanofibrillar network. SEM images of (d) a PVA hydrogel and (f) a PVA organohydrogel (scale bar: 1  $\mu\text{m}$ ). Atomic force microscopy (AFM) height images of (e) a PVA hydrogel and (g) a PVA organohydrogel (scale bar: 500 nm). Reproduced with permission.<sup>52</sup> Copyright 2020, American Chemical Society.

induces the aggregation and crystalline domains in the nanofibrils by phase separation, which can effectively delay the fracture of individual fibrils by crack-pinning. Similarly, a nanofibrillar PVA organohydrogel cross-linked by numerous PVA nanocrystallites was formed by freeze-thaw and solvent replacement (Fig. 9b-g).<sup>52</sup> Thanks to the generation of nanoscale PVA crystalline domains induced by Gly, excellent mechanical properties are achieved accordingly. However, the PVA hydrogel sample exhibits microfibrillar morphology in the absence of Gly, and shows a very low mechanical strength and relatively low elongation at break.

### 3.2. Conductivity

A good conductivity in organohydrogels is generally required in most application areas, such as sensors, nanogenerators, and storage devices. As for hydrogels, the large amount of water contained facilitates ion transporting within the network and makes them capable of transmitting electronic signals.<sup>145,146</sup> Although the conductivity is reduced after the replacement of free water, the anti-freezing and water retention ability achieved in organohydrogels can also stabilize their conductivity even under harsh conditions. Various methods have been developed to improve the conductivity of organohydrogels. At present, the simplest and most effective method is to directly introduce ions into the organohydrogel, which is achieved by using polyelectrolytes or adding inorganic salts. The polyelectrolyte network can release large numbers of free-moving ions into the solvent water, thereby achieving a good ionic conductivity.<sup>43,94</sup> Yang *et al.* prepared a conductive organohydrogel with sodium methacrylate (MAANa) and [2-(methacryloyloxy)-ethyl] trimethyl ammonium chloride (DMC) as monomers, which exhibited a good conductivity even in low-temperature environments.<sup>15</sup> Moreover, the conductivity of this organohydrogel was not affected by current frequency and had the potential to be used as signal transmission materials.

Nowadays, various inorganic salts including KCl,<sup>63,87,147</sup> NaCl,<sup>88,95</sup> LiCl,<sup>42,148</sup> and AlCl<sub>3</sub>,<sup>64,67,119</sup> have been introduced into organohydrogels to increase their ionic conductivity. The addition of salt can be achieved by directly mixing the salt in the precursor solution or immersing the prepared gel in the salt solution for the ions to diffuse into the network. Accordingly, the conductivity will increase with the salt concentration due to the increased dissociated ion concentration, suggesting the contribution of the added ions to the conductivity. However, this increase in conductivity has an upper limit. Ye *et al.* proposed that excess salt in the organohydrogels will form ion pairs or clusters rather than existing as dissociated ions, resulting in no longer increased conductance.<sup>95</sup> In particular, as mentioned before, the introduction of ionic polymers or salts into organohydrogels is also beneficial to the antifreeze ability of the materials, which can effectively compensate for the contradiction between conductivity and frost resistance.<sup>15</sup>

The conductivity of organohydrogels is not only related to ion concentration, but also largely depends on the mobility of ions. Generally, a polymer network with a high degree of cross-linking is not conducive to ion migration;<sup>149</sup> that is, there is a dilemma between strength and ionic conductivity in hydrogels.

Another typical strategy is to introduce a secondary conductive network into the traditional organohydrogel, such as conductive polymers,<sup>49,132</sup> CNFs,<sup>95</sup> MXene nanosheets,<sup>23,70</sup> and CNTs,<sup>16,84</sup> which may contribute to the increase in mechanical strength and conductivity simultaneously. The conductive polymer is a kind of functional polymer with highly conjugated polymer chains; it has active  $\pi$ -bonded electrons and can provide channels for carrier transfer and transition, and has intrinsic electronic conductivity.<sup>150-152</sup> However, conductive hydrogels based on conductive polymer matrices, such as PANI, polypyrrole, and PEDOT, tend to have lower strength and flexibility, and thus they are usually selected to be incorporated into another polymer matrix.<sup>84,153</sup> For example, Rong *et al.* reported a PVA organohydrogel with adjustable conductivity by adding PEDOT: PSS.<sup>49</sup> As for CNFs, the negative surface carboxylate groups on them can attract counter ions and provide more hopping sites for their migration,<sup>95,154-156</sup> thus leading to an increase in the conductivity. MXene nanosheets possess superior electrical conductivity, rich surface functional groups, good hydrophilicity, and correspondingly good dispersibility, which will undoubtedly show tremendous potential in the fabrication of organohydrogels with stable electrical properties.<sup>157-159</sup> For example, Wei *et al.* developed a nanocomposite organohydrogel by incorporating conductive MXene nanosheets and TA@CNFs into the polymer networks, which demonstrated outstanding flexibility and electrical conductivity within a wide temperature range.<sup>23</sup> Herein, MXene is connected to the organohydrogel matrix to form a conductive skeleton, and thus endows the organohydrogel with high electrical conductivity. Similarly, the introduction of CNTs with high conductivity and specific surface area can also benefit the improvement of conductivity,<sup>16</sup> but their aggregation problem needs to be solved first.

### 3.3. Self-healing ability

As a wearable electronic device, organohydrogels will suffer unavoidable damage during the repeated stretching and bending, including cracks, crazing, puncture, and delamination, which will lead to a sharp degradation in the mechanical and electrical properties of the device. Therefore, self-healing organohydrogels that can self-repair some unexpected damages have a wider application field and longer service life, reducing resource waste. Mechanical damage of the gel network will cause the polymer chains to break and slip with each other, and leave active groups on the broken interfaces.<sup>5</sup> In general, as seen in Fig. 10, the intrinsic self-healing process is realized by the diffusion and rearrangement of molecules and inherently reversible chemical bonding between molecular chains<sup>160,161</sup> and controlled by thermodynamics or reaction kinetics.<sup>162</sup> When a break occurs, the entropy increase of the system and the gradient of the molecular chain network density will drive the chain to spread.<sup>163</sup> Specifically, the flexibility of the polymer chain will strongly affect chain diffusion across a fracture surface interface, and often the polymer chains with a low molecular weight and a low glass transition temperature show relatively high flexibility and correspondingly high molecular diffusion speed.<sup>164</sup> When the driving force of the system is not enough, the healing process of

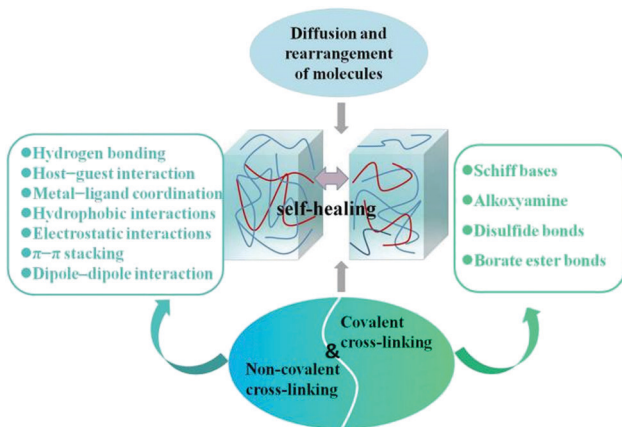


Fig. 10 Schematic illustration of the self-healing mechanisms.

the gel needs external energy to proceed, such as high temperature<sup>165,166</sup> and ultraviolet irradiation.<sup>167,168</sup>

The subsequent self-healing process is mainly realized by dynamic covalent cross-linking and non-covalent cross-linking.<sup>69</sup> Non-covalent cross-links used to achieve self-healing properties mainly include hydrogen bonding,<sup>15,169,170</sup> host-guest interaction,<sup>171–173</sup> and metal-ligand coordination.<sup>164,174,175</sup> Hydrogen bond is a common reversible weak bond in polymer networks, which can automatically re-bond to repair damage even at room temperature. Hydrogen bond-based self-healing was first proposed in rubber. It can restore damage with the help of multiple hydrogen bonds in molecular chains and does not require any external assistance.<sup>176</sup> Therefore, compared with hydrogels, the abundant hydrogen bonds formed between organic molecules and polymer networks make organohydrogels show better self-healing ability.<sup>49,87</sup> The host-guest supramolecular interactions originate from the complementary guest and host moieties in polymer networks, such as cyclodextrins and ferrocene molecules<sup>171</sup> or cyclodextrin and azobenzene molecules,<sup>172</sup> which can form host-guest inclusion complex due to the high affinity between them. When damage occurs, the damaged surface will expose the dangling host and guest molecules, which can autonomously recognize each other and recombine again to repair the damaged surface through the dynamic host-guest interactions. In particular, since the affinity between host and guest molecules can be controlled by external stimuli, these host-guest supramolecular hydrogels can be used in switch soft materials.<sup>171</sup> Metal-ligand bonds possess moderate bond energy, which can dynamically associate or dissociate at room temperature and thus endow the hydrogel with self-healing properties. Besides these, other non-covalent supramolecular interactions such as hydrophobic interactions,<sup>177,178</sup> electrostatic interactions,<sup>179,180</sup>  $\pi$ - $\pi$  stacking<sup>181–183</sup> and dipole-dipole interaction,<sup>184</sup> which can be introduced by modifying hydrophobic blocks, charged groups, or surfactant molecules in polymer networks, have also been reported to be used in the preparation of self-healing materials. These reversible breakable bonds can provide an energy dissipation mechanism to prevent the breaking of the molecular backbone and realize subsequent self-healing of damaged materials.<sup>185</sup>

As for the self-healing mechanism based on covalent cross-linking, various reversible covalent bondings such as Schiff bases,<sup>186,187</sup> alkoxyamine,<sup>188</sup> disulfide bonds,<sup>189,190</sup> and borate ester bonds<sup>23,43</sup> have been studied for achieving self-healing properties. Synergistically, high healing efficiency and speed can be achieved by combining these two mechanisms. For example, Wu *et al.* reported a MXene nanocomposite organohydrogel modified with dopamine (DA) and phenylboronic acid (PBA), and its good self-healing capability is mainly attributed to the existence of abundant dynamic hydrogen bonds and covalent ester bonds.<sup>70</sup> The organohydrogel can re-ignite the LED when the two cut parts are brought together, and the stretch strain can be restored to 88.75% after self-healing for 12 h (Fig. 11). For most self-healing organohydrogels, their self-healing process can mostly be carried out at room temperature, and the recovery speed of electrical and mechanical properties is quite different. Generally, their conductivity can be restored within a few seconds because the physical dynamic cross-linking at the fracture interface can quickly reform at room temperature, and the self-healing of mechanical properties is relatively slow due to the rearrangement of the polymer matrix, which can be further accelerated by increasing the temperature. In particular, the healing process of some organohydrogels requires a heating and cooling cycle. For example, for a carrageenan-based organohydrogel, the self-healing of its mechanical properties is largely derived from the dissociation of the double-helical structure of carrageenan at high temperatures and the reformation at low temperatures.<sup>63,87</sup> Alternatively, when there are crystalline domains in an organohydrogel, the self-healing also needs to undergo a heat treatment.<sup>49</sup>

Nowadays, the self-healing ability at low temperatures is very promising, but there are huge challenges to be addressed. The realization of the self-healing ability at sub-zero temperature is limited by the slowing down of molecular chain movement and the retarded reconstruction of interfacial reversible bonds.<sup>132,191</sup> Although few antifreeze hydrogels that self-heal through weak



Fig. 11 The self-healing ability of organohydrogels: (a) the self-healing process of the mechanical properties for the MXene nanocomposite organohydrogel after cutting. (b) The green LED connected in series with the organohydrogel serves as an indicator of the conductivity in the self-healing process. Reproduced with permission.<sup>70</sup> Copyright 2020, Royal Society of Chemistry.

hydrogen bonding, host-guest structure, or electrostatic interactions at low temperatures have been reported, their self-healing process is usually time-consuming.<sup>132,192</sup> For organohydrogels, their polymer chains still have a good fluidity at sub-zero temperatures, making it possible to self-heal at low temperatures.<sup>43,132</sup> Attractively, Borax chemistry is an effective method to achieve remarkable self-healing ability. Due to the incorporation of sufficient, fast-forming, and temperature-insensitive borate bonding sites, it ensures a high interfacial bonding density, and thus achieves a fast self-healing process even at low temperatures.<sup>132,193,194</sup> Driven by this, a DN PAA-PVA organohydrogel combined with a high content of borax displayed an outstanding self-healing capability even at an ultralow temperature of  $-60\text{ }^{\circ}\text{C}$ , and the cut specimens could self-heal within 1 minute of contact due to the cross-linking of borax with PVA and EG solvent.<sup>43</sup>

### 3.4. Adhesiveness

The stable contact of an organohydrogel with biological tissues can make it have the potential to be used in portable and wearable electronic devices, which means that good cohesion and adhesion should be displayed in an organohydrogel.<sup>195,196</sup> The cohesion of the polymer network is related to its mechanical properties, and the corresponding cohesion strength can be evaluated by measuring the elastic modulus.<sup>197,198</sup> In the past, hydrogels needed the help of external adhesives to bond on the substrate, such as bandages, scotch tapes, or 3M adhesives.<sup>199,200</sup> They generally possess good stickiness, but they can't adapt well to uneven surfaces and have poor air permeability, which is not conducive to sticking to the skin for a long time. In particular, when they are applied to the detection of biological signals such as electromyography (EMG) and electrocardiography (ECG), the obvious layered structure will lose the accuracy and durability of detection to a certain extent. Therefore, there is an important requirement for the development of organohydrogels with self-adhesive ability, which requires that the organohydrogels can easily and strongly adhere to various substrates without requiring extra agents, so as to achieve high accuracy of information acquisition.

Nowadays, various strategies have been developed to prepare self-adhesive organohydrogels by introducing adhesive components (chitosan, nucleobases, and proteins) or functional groups in the polymer network.<sup>84,201,202</sup> These functionalized organohydrogels can form covalent or non-covalent interactions with the surrounding surfaces to achieve durable and repeatable adhesion.<sup>15,23,43,55,64,88,132</sup> Generally speaking, many adhesions based on reversible non-covalent interactions can experience multiple adhesion cycles without damaging the material and loss of adhesion strength.<sup>203,204</sup> For example, Qin *et al.* proposed a supramolecular organohydrogel with excellent adhesive properties at various substrate surfaces, which could be attributed to the synergetic interactions of hydrogen bonding, electrostatic interaction, and metal complexation between the organohydrogel and substrates.<sup>55</sup> In particular, it can maintain such good adhesiveness even at  $-70\text{ }^{\circ}\text{C}$  due to its good frost resistance, which is superior to those of current adhesive

hydrogels and facilitates its practice applications in actual harsh environments. Also, the adhesiveness at higher temperatures is indispensable in a specific environment, and it is mainly related to the thermal stability of the polymer network. In addition, the adhesion based on covalent interaction is also explored and is generally stronger due to the high energy of chemical bonds, such as Schiff bases<sup>205</sup> and disulfide bonds.<sup>206</sup> Recently, Niu *et al.* reported an environmentally compatible gelatin/poly(AA-N-hydrosuccinimide ester) (PAA-NHS ester)-based organohydrogel.<sup>207</sup> This organohydrogel demonstrated strong adhesion on the skin even underwater because of the introduction of multiple interactions, including hydrogen bonds, electrostatic interactions, and covalent cross-linking between the NHS ester from the gel and amino groups from human skin (Fig. 12).

To date, new adhesive materials inspired by nature's biological adhesion properties have been continuously developed. For example, inspired by glutinous rice, Zhou *et al.* developed a poly(AA-co-AM) organohydrogel by introducing amylopectin (AP) into the polymer network, which showed outstanding adhesion properties in a wide working range ( $-20$  to  $80\text{ }^{\circ}\text{C}$ ) due to the



Fig. 12 The adhesive performance of organohydrogels: (a) adhesion of an organohydrogel on the skin surface. (b) The T-peeling test shows the presence of strong adhesion between the organohydrogel and PDMS. (c and d) The interfacial adhesion properties between an organohydrogel and porcine skin under normal and underwater conditions. (e) Schematic diagram and (f) photographs of the lap-shear test between an organohydrogel and PDMS. (g) Schematic diagram and (h) photographs of 90° peeling tests between an organohydrogel and a wet human skin. Reproduced with permission.<sup>207</sup> Copyright 2021, John Wiley and Sons.

abundant free hydroxyl groups in AP.<sup>208</sup> It is worth noting that underwater adhesion or wet adhesion is the biggest challenge for hydrogel materials. When liquid is present, a hydration layer will be formed on the surface of the adhesive material, which causes the dissolution of the adhesive molecules and prevents them from bonding with other surface groups, resulting in poor adhesion.<sup>209,210</sup> Mussels are aquatic organisms with excellent adhesion properties. They secrete byssus composed of viscous proteins so that they can be firmly attached to various surfaces in dry or even in humid environments.<sup>84,211,212</sup> The adhesion mechanism of mussels mainly involves the secreted viscous protein rich in dihydroxyphenylalanine (DOPA) residues with catechol groups, which can form chemical bonds and hydrogen bonds with polar surfaces to achieve adhesion. Besides, the catechol group of DOPA tends to be oxidized to reactive quinone moieties, causing cross-linking between proteins and strong cohesion.<sup>28,213</sup> Moreover, the oxidized quinone moieties can also form covalent bonds with the diverse nucleophilic groups (*e.g.*, amines, thiols, and imidazoles) on biological tissues to establish a strong adhesion.<sup>214,215</sup> Based on this, several mussel-inspired adhesive organohydrogels have been developed by incorporating or modifying additives containing catechol groups in the polymer network. For example, PDA is often incorporated into organohydrogels to enhance self-adhesiveness due to the abundant presence of catechol groups.<sup>28,216</sup> Han *et al.* developed a conductive nanocomposite organohydrogel that exhibited excellent tissue adhesiveness due to the modification of muscle-inspired PDA on CNTs.<sup>84</sup> However, DA is difficult to be oxidized to PDA in a binary solvent of organohydrogels, and it requires additional oxidation before gelation, which increases the preparation steps.<sup>217</sup>

The tunicate mimetic adhesive system can also inspire the preparation of viscous organohydrogels due to the abundant pyrogallol moiety,<sup>64,209</sup> which can also form strong interactions with diverse surfaces and provide strong cohesion for polymer networks.<sup>218,219</sup> Natural pyrogallol derivatives, such as gallic acid and TA, are cheaper than catecholic compounds and have more abundant reserves.<sup>220–222</sup> Compared with the catechol group, the pyrogallol group has a higher binding affinity with the proteins or metal ions,<sup>223,224</sup> resulting in better adhesion properties. For example, Wei *et al.* reported a conductive nanocomposite organohydrogel incorporating TA modified CNTs,<sup>23</sup> which exhibited an excellent self-adhesiveness with high adhesive strength applicable to diverse surfaces. Moreover, there are more adhesion mechanisms inspired by nature that can continue to be used in the preparation of organohydrogels with excellent adhesion properties. van der Waals forces and capillary forces are very promising interactions to achieve adhesion, and the gecko is a good example in nature.<sup>6,225</sup> Therefore, in addition to the changes in components that need to be considered when designing organohydrogels, microstructure adjustment is also the key to material functionalization.

Taking into account the solvent resistance of heterogeneous organohydrogels, underwater adhesion can also be achieved by introducing hydrophobic polymers without modification of additional surface groups. Liu *et al.* prepared a solvent-resistant and non-swelling heteronetwork organohydrogel through the

copolymerization of MEA and AA in a mixed solvent of H<sub>2</sub>O/DMSO.<sup>45</sup> The organohydrogel exhibited robust adhesion properties in organic and aqueous solutions due to the synergistic hydrophobic and hydrophilic components. Specifically, the hydrophilic segments in the gel can effectively resist the corrosion of organic solvents and achieve underwater adhesion. When the organohydrogel is immersed in water, water molecules can enter the polymer network by displacing the interior DMSO molecules. Meanwhile, the corresponding precipitation and association of the hydrophobic segments can lead to mutual repulsion between water molecules and the organohydrogel and simultaneously increase the cohesion for strong underwater adhesion. Besides, a programmable adaptive adhesion was achieved by introducing thermoelectric components in the heterogeneous organohydrogel to reversibly transform to a more compliant and deformed state to match the rough surface morphology, due to their thermomechanical performance.<sup>80</sup> Nevertheless, underwater adhesion and programmable adhesion still need further exploration in the future.

### 3.5. Others

In addition to the common characteristics mentioned above, organohydrogels need to be developed with more functionalities by modifying some functional molecules to be applied in specific fields, such as antibacterial activity, biocompatibility, degradability, thermoplasticity, transparency, fluorescence, *etc.*

The antibacterial activity appears to be particularly important when the organohydrogel is in contact with biological tissues, because the humid environment of the organohydrogel will inevitably lead to the breeding and growth of a large number of bacteria. Commonly, various antibacterial substances have been introduced into the gel material to obtain antibacterial activity, such as silver nanoparticles,<sup>226</sup> antibiotics,<sup>227</sup> fullerene,<sup>228</sup> and Al<sup>3+</sup>.<sup>119</sup> However, the release of such antibacterial substances will seriously affect the long-term antibacterial properties, and even cause metal-ion toxicities and allergic reactions,<sup>229–231</sup> which is adverse to its application in biological tissues. In addition to this, antibacterial activity can also be achieved by changing the surrounding environment of the bacteria, such as temperature<sup>232–234</sup> and pH.<sup>235</sup> For instance, incorporating photothermal agents in the organohydrogel can cause the denaturation of bacterial proteins by converting light into local heating to impart organohydrogels with an excellent and broad-spectrum photothermal sterilization ability.<sup>236,237</sup> Beyond that, positively charged materials are generally considered to possess good antibacterial properties, such as ionic liquids,<sup>69</sup> quaternary ammonium salt,<sup>238</sup> *etc.*, which can be accumulated and adsorbed on the negatively charged bacterial walls through electrostatic force to change the charge of the bacterial cell surface and damage the membrane structure of bacterial cells, thus causing growth inhibition and death of bacteria.<sup>239–242</sup> Considering the toxicity of these substances, some non-toxic and inherently antibacterial substances containing numerous positively charged chemically groups, such as chitosan<sup>243</sup> and  $\epsilon$ -polylysine,<sup>53</sup> also show a good long-term antibacterial activity and do not cause additional harm to humans. In particular, biocompatibility is the primary



consideration for the application of organohydrogels *in vivo*, which requires that the materials do not have toxicity or initiate foreign body responses in biological tissues. However, the initiators, cross-linkers, organic solvents, and unreacted monomers frequently used in the preparation of organohydrogels are mostly toxic. Therefore, organohydrogels with excellent biocompatibility need to avoid free radical polymerization and are usually based on natural polymers or FDA-approved polymers.<sup>173</sup>

There are millions of tons of e-waste accumulated here every year, which is contrary to the concept of sustainable development and causes serious economic and environmental problems.<sup>244</sup> In order to alleviate these problems, on the one hand, degradable “green” electronic devices need to be developed. Compared with traditional hydrogels based on chemical cross-linking, many natural material-based hydrogels or physically cross-linked hydrogels (agarose, gelatin, alginate, PVA, *etc.*) can be entirely degradable without producing any toxic substances.<sup>88,245</sup> Similarly, the hydrogel network formed by other weak bonds such as metal-ion coordination or electrostatic interactions is relatively easy to dissociate under certain conditions to achieve degradability.<sup>124,246–248</sup> Unfortunately, the introduction of the ability to degradable usually needs to be done at the cost of compromising performance. Degradable hydrogels usually have poor

mechanical properties and long-term stability due to weak cross-linking bonds. To address this problem, Baumgartner *et al.* reported an organohydrogel based on naturally occurring materials that can be completely degraded when treated in wastewater.<sup>235</sup> Its mechanical properties can be well maintained for more than one year under ambient conditions by using hydrophobic biodegradable coating strategies based on shellac resins. The degradation of the encapsulation layer is triggered in an alkaline solution, which subsequently leads to the complete degradation of the biogel. This may open the way for the application of degradable gels in water or *in vivo*. It should be noted that the simple dissolution of polymers cannot reduce environmental problems, and may cause harm through accumulation in filtration systems such as the kidneys.<sup>249</sup> On the contrary, a more complete chemical degradation of a single polymer chain is harmless to the human body and the environment.<sup>250</sup> On the other hand, reusable electronics can also be developed to reduce e-waste. Generally, organohydrogels with good recyclability or thermoplasticity are composed of reversible non-covalent interactions, which allows them to reform easily into different shapes as required.<sup>55,120,121</sup> Unlike degradation, it does not require to destroy the long molecular chains of the polymer. Inevitably, the mechanical properties of the remolded gel network will slightly decrease.

**Table 3** Summary of various functionalities of diverse organohydrogels

Materials	Electro-mechanical properties (maximum strain, tensile strength, conductivity)	Adhesiveness (substrate)	Self-healing (healing efficiency)	Transparency	Antibacterial ability	Biocompatibility/ degradability	Thermoplasticity (remoldability)
PVA/carbon black (CB)/CNT organohydrogel <sup>91</sup>	643.2%, 4.8 MPa, $10^5 \Omega$	—	64.9% (stress) 60.1% (strain)	—	—	—	Yes
PAM/montmorillonite/CNT organohydrogel <sup>66</sup>	4400%, 170 KPa, $10^{-5} \text{ S cm}^{-1}$	—	—	—	—	—	—
Gelatin supramolecular organohydrogel <sup>55</sup>	690%, 3 MPa, —	150 KPa (copper)	50% (tensile strength)	Yes	—	—	Yes
TA@CNF/MXene/PAM organohydrogel <sup>23</sup>	1500%, 156.5 KPa, $2 \text{ mS cm}^{-1}$	117 $\text{N m}^{-1}$ (wood)	Yes	—	—	—	—
PAM/carrageenan DN organohydrogel <sup>87</sup>	950%, 417 KPa, 15 $\text{k}\Omega$	—	Yes	Yes	—	—	—
Nanofibrillar PVA organohydrogel <sup>52</sup>	390%, 1.4 MPa, —	—	—	90%	—	Biocompatibility	—
P(MAANA-DMC) organohydrogel <sup>15</sup>	2000%, 56 KPa, $10^{-2} \text{ S cm}^{-1}$	2.5 kg (PTFE)	96% (conductivity)	—	—	—	—
PAAM-Clay organohydrogel <sup>256</sup>	3310%, 0.25 MPa, $\sim 10^5 \Omega$	—	95% (conductivity)	—	—	—	—
PDA-CNTs/PAM/PAA organohydrogel <sup>84</sup>	700%, 70 KPa, $8 \text{ S m}^{-1}$	57 KPa (porcine skin)	—	—	—	—	—
PVA/SNF/CN organohydrogel <sup>119</sup>	585.8%, 1.39 MPa, —	—	—	—	Yes	—	Yes
PVA/CNF organohydrogel <sup>95</sup>	660%, 2.1 MPa, $3.2 \text{ S m}^{-1}$	—	—	90%	—	—	—
Alginate/PEGDA organohydrogel fibers <sup>74</sup>	400%, 200 KPa, $0.765 \text{ S m}^{-1}$	—	—	Yes	—	—	—
PVA-TA@talc organohydrogel <sup>71</sup>	750%, 550 KPa, —	—	—	UV-filtering	—	—	—
PVA-borate-TA-CNTs organohydrogel <sup>120</sup>	180%, 450 kPa, —	—	98% (strain)	—	—	—	Yes
Gelatin-based biogel <sup>237</sup>	254%, 1.86 MPa, —	Yes	Yes	—	Yes	Degradability	—
$\epsilon$ -PL-gelatin-PAM organohydrogel <sup>53</sup>	1400%, 300 KPa, —	181.6 KPa (hogskin)	—	—	Yes	Biocompatibility	—
Poly(AA-co-AM)/AP organohydrogel <sup>208</sup>	1089%, 200 KPa, $0.2 \text{ S m}^{-1}$	22.18 KPa (copper)	—	90%	—	—	—

When it comes to optical performance, good transparency can not only realize the visualization of the internal conditions of the wearable electronic devices and the skin during the operating process, but also shows great application potential in military camouflage, optometry products, and display applications.<sup>52,251</sup> In the organohydrogel, the incorporation of organic agents can well hinder the phase separation of the polymer or lead to the formation of smaller polymer crystallites,<sup>95,121</sup> thereby reducing the interference to light and obtaining higher transparency. Additionally, similar to hydrogels, a fluorescent organohydrogel can also be developed by modifying fluorescent monomers on the polymer network, and it can show a dynamic color or brightness change in response to external stimuli through appropriate molecular design.<sup>252,253</sup> For example, Chen *et al.* developed a heterogeneous organohydrogel with simultaneous fast morphing and fluorescent changes in response to temperature by modifying the fluorescent monomer *N*-(4-(1,2,2-triphenylvinyl)phenyl)acrylamide (ATPE) and the fluorescent ligand 6-acrylamidopicolinic acid (6APA).<sup>252</sup> Specifically, the fluorescence intensity of ATPE on the hydrophobic chains can increase sharply when the temperature increases, showing an aggregation induced emission (AIE) behavior. And 6APA can combine with  $\text{Eu}^{3+}$  to form the 6APA- $\text{Eu}^{3+}$  complex that can emit red fluorescence, and its coordination degree also changes with temperature, resulting in a change in fluorescence color.

As demonstrated above, stretchable organohydrogels can be endowed with abundant functionality through unique functional monomers and exquisite structural design, leading to the possibility of their application in various fields. Here we summarize the various properties of some representative organohydrogels reported recently and they are displayed in Table 3. Notably, it is difficult for the existing organohydrogels to achieve a satisfactory balance among the above-mentioned performance. Thus, there are still great challenges in realizing multifunctional organohydrogels. More importantly, in addition to optimizing these properties, some novel functionalities are also expected to be continuously developed in organohydrogels by compounding with other functional materials, such as electromagnetic shielding capabilities, X-ray absorption, photoelectric conversion capabilities, *etc.* Impressively, considering the coexisting hydrophilic and hydrophobic networks of heterogeneous organohydrogels, they are easier to modify these additives with different hydrophilicities and thus can serve as excellent functional carriers with better manipulation and less restriction.

## 4. Application for organohydrogels

### 4.1. Sensors

In the past, sensor research was mainly based on inorganic nanomaterials, such as metal oxide semiconductors,<sup>254–256</sup> transition metal dichalcogenides,<sup>257–259</sup> and carbon nanomaterials.<sup>260–262</sup> Despite achieving excellent sensitivity, their stretchability is limited. In contrast, a conductive organohydrogel also has the ability to convert specific external stimuli (such as strain, pressure, temperature, humidity, gas, *etc.*) into electrical signals that can be detected, resulting in a significant change in resistance or



Fig. 13 Strain sensors for real-time monitoring of various human motions: recognition of different bending states of (a) fingers, (b) elbows and (c) knees; (d) walking monitoring; (e) pulse detection; and (f) voice recognition. Reproduced with permission.<sup>95</sup> Copyright 2020, John Wiley and Sons.

capacitance in the macroscopic view. This means that organohydrogel can be widely exploited as a multi-functional wearable sensory system in human-machine interface, human health detection, motion detection, and other fields, showing a wide operating temperature range.

Strain sensor is a very important type of sensor, which can respond to mechanical deformation and be used for real-time monitoring of various human motions (Fig. 13).<sup>95,121</sup> So far, a large number of antifreeze and durable strain sensors based on organohydrogels have been developed. For ion-conductive organohydrogels, the change in electrical signal during stretching is mainly due to the elongated ion transmission pathway.<sup>4</sup> In addition, the density of the polymer chain also has an impact on the transport of ions. When a moderate deformation is applied, the polymer chain will unfold accordingly to weaken the hindering effect of the polymer network on ion transportation. However, when excessive stress is applied, the partial rupture of the polymer network will hinder the transport of ions, resulting in a decrease in electrical resistance. For electron-conductive nanofiller incorporated organohydrogels, electrons are transported by forming an interconnected three-dimensional conductive pathway in the polymer network. During the stretching process, the variation of the electrical signal is closely related to the rearrangement of the conductive network.<sup>66</sup> Under small tensile strains, the distance between nanofillers will gradually increase, increasing the electrical resistance. As the strain gradually increases, part of the conductive components will gradually separate and obviously damage the conductive channels, leading to a sharp increase in resistance. For organohydrogels, in which both ions and electrons participate in conduction, the change in resistance is related to the changes of both the ion transporting pathway and the electronic conduction channel during stretching. It is worth noting that the degree of resistance change caused by stretching under different strain ranges is different due to the domination of different response mechanisms. Thus, the response of organohydrogels *versus* strain relationship generally shows two or three linear regions.

Nowadays, strain sensors based on conductive organohydrogels have two main challenges, including the realization of a

wide linear strain range and high sensitivity. The detection of a small strain endows the sensor the ability to detect subtle human motions, such as pulse, micro-expression, vocalization, *etc.*<sup>263</sup> Generally, the polymer network incorporating nanofillers has better sensitivity under a small strain, because the contact of rigid nanofillers will be quickly destroyed under tension.<sup>264</sup> Equally important, the detection of moderate and high strains is also of great significance in practical applications, and a wide linear strain range is usually achieved by improving the mechanical properties of the gel. Recently, Sun *et al.* reported a conductive nanocomposite organohydrogel as a wearable strain sensor with good environmental tolerance,<sup>66</sup> which exhibits satisfactory sensitivity and an ultrawide strain sensing range (0–4196%) due to the remarkable mechanical and electrical properties (Fig. 14a and b). The sensitivity of an organohydrogel to strain is evaluated by the gauge factor (GF), which is calculated from the slope of the relative resistance change ( $(R - R_0)/R_0$ ) versus the applied strain curve.<sup>23,95</sup>

Generally speaking, higher GF values are obtained by increasing the original conductivity of organohydrogels, which results in more excellent signal acquisition capabilities. Based on this, various salts and conductive nanofillers should be introduced into the gel to construct conductive channels that are more easily altered. Representatively, Wu *et al.* used PAM/carrageenan/KCl organohydrogels to construct an ultrastretchable strain sensor with a GF of 6; various human motions can be detected even at  $-18\text{ }^\circ\text{C}$  or after exposure to ambient air for as

long as nine months (Fig. 14c–h).<sup>87</sup> Wei *et al.* developed a nanocomposite organohydrogel based strain sensor with a GF of 8.5 by introducing a conductive network framework formed by interconnecting MXene nanosheets,<sup>23</sup> while most of the GF values of hydrogel-based strain sensors reported in the past are only around 2.<sup>265,266</sup> Attractively, Ge *et al.* reported a muscle-inspired organohydrogel-based strain sensor with a high GF of 18.28 by mimicking the fiber-reinforced laminated nanocomposites and “sense-transfer-process” pattern,<sup>132</sup> and this superior electro-mechanical response is attributed to a disconnection mechanism and tunneling effect in sensors. Moreover, Han *et al.* prepared an ultra-sensitive strain sensor (GF = 343) with anti-freezing and anti-drying ability by introducing tightly cross-linked CNT films on the surface of organohydrogels; this strategy had great advantages of combining high sensitivity and a relatively wide detection range.<sup>267</sup> Inspired by this, the replacement of CNTs with other conductive one-dimensional nanomaterials such as Ag nanowires can also lead to an ultra-high response.

Similarly, the compression of organohydrogel will also cause changes in electrical signals, which means that it can also be used in practice as a flexible pressure sensor. Distinct from the traditional electron-conductive metals and inorganic semiconductors, a pure ion-conductive organohydrogel exhibits a smaller change in resistance under compression due to the limited changes in the ion transport pathway.<sup>157,268,269</sup> Hence, flexible pressure sensors are usually constructed using electron-conductive nanofiller incorporated organohydrogels to realize

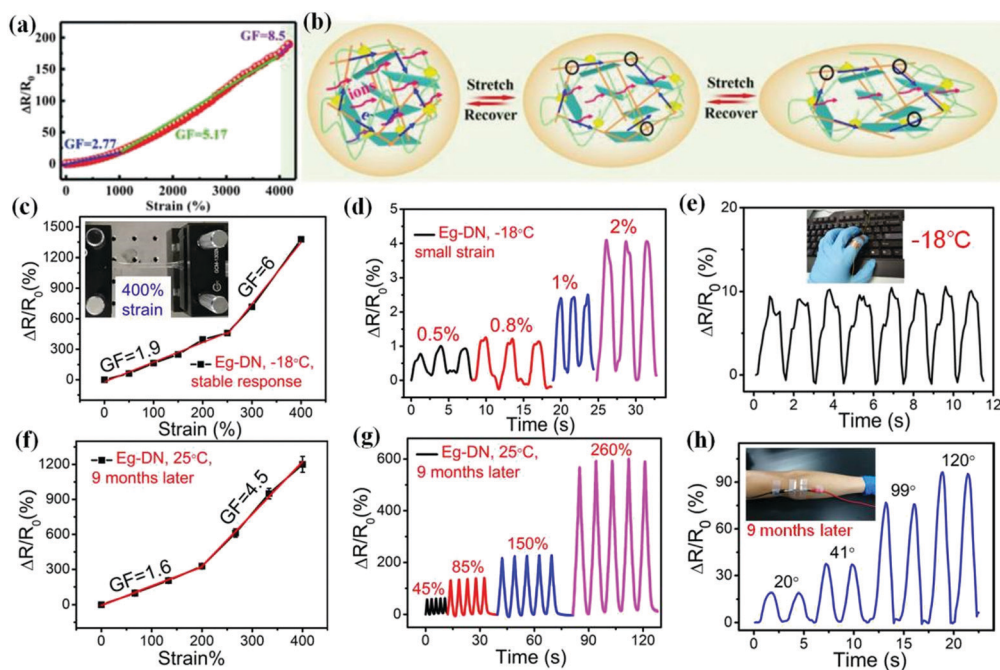


**Fig. 14** The strain sensing performance of an organohydrogel-based sensor: (a) the relationship between the  $\Delta R/R_0$  value and the applied strain and (b) the schematic diagram of the sensing mechanism for a conductive nanocomposite organohydrogel-based strain sensor. Reproduced with permission.<sup>66</sup> Copyright 2021, John Wiley and Sons. (c) Response–strain curve of the PAM/carrageenan/KCl organohydrogel-based strain sensor at  $-18\text{ }^\circ\text{C}$ . (d and e) The dynamic response curve of the sensor to different small strains (0.5–2%) or finger tapping on the keyboard at  $-18\text{ }^\circ\text{C}$ . (f) Response–strain curve of the PAM/carrageenan/KCl organohydrogel-based strain sensor after placing in ambient air for 9 months. (g and h) The dynamic response curve of the sensor to different strains (45–260%) or elbow joint bending after exposure to ambient air for 9 months, showing an excellent environmental adaptability and durability. Reproduced with permission.<sup>87</sup> Copyright 2019, American Chemical Society.

higher pressure sensitivity. For instance, Zheng *et al.* developed a conductive organohydrogel composed of thioctic acid, borate, CNTs, and PVA, which presented a high conductive sensitivity ( $0.625 \text{ KPa}^{-1}$  for 0–6 KPa) even at  $-40 \text{ }^\circ\text{C}$ .<sup>120</sup> To further improve the pressure sensitivity, piezoelectric materials such as polyvinylidene fluoride (PVDF) and  $\text{BaTiO}_3$  nanoparticles,<sup>270</sup> can be incorporated into organohydrogels to obtain additional electrical responses derived from the piezoelectric effect.<sup>271,272</sup> Structurally, the pressure response of the organohydrogel with a nanofiber stacking structure is significantly improved compared to that of the conventional thin-film structure due to stress concentration.<sup>273,274</sup> The broad pressure detection range is also another important performance indicator that the flexible pressure sensor needs to continuously strive to achieve. The thought is to build an elastic gel network to improve the deformation-tolerant performance of the material so as to achieve a wide pressure range.<sup>35</sup> Moderate compressive strength and modulus are required to make the material neither too brittle nor too soft.

Furthermore, there are some other performance indicators in strain or pressure sensors that need to be optimized, including response/recovery speeds, reversibility, stability, and durability. On the one hand, the fast response speed is conducive to real-time and accurate sensing. However, most of the existing strain sensors cannot meet this detection requirement due to the hysteresis, and are unsuitable for continuous monitoring of high-speed and high-frequency motion. To address this problem, Song *et al.* prepared organohydrogel fibers with excellent elasticity resulting from the predominantly covalently crosslinked network, which exhibits negligible hysteresis during the tensile test and can accurately capture high-frequency (4 Hz) and high-speed ( $24 \text{ cm s}^{-1}$ ) motion of a simulated engine.<sup>74</sup> On the other hand, the reversible, stable, and long-lasting response of the sensor to strain/pressure is also the key to considering whether it can be used in actual production. In general, thanks to the organic solvent contained in the organohydrogel, the organohydrogel-based strain/pressure sensors can exhibit good durability and operate under various harsh conditions.<sup>64,73,91,119</sup>

Temperature sensor is another essential wearable device that can be used for real-time monitoring of human physiological signals.<sup>275,276</sup> In general, for ion-conductive gels, the variation of temperature will change ion mobility and correspondingly cause changes in resistance. Additionally, ion concentration in the migration pathway will increase with temperature due to the dissociation of the ion pair bonded on the polymer chain, resulting in an increase in conductivity.<sup>277</sup> Moreover, the thermal movement of the polymer chain accelerates as the temperature increases, resulting in a weakened polymer's hindering effect on ion transport and can also significantly reduce electrical resistance. Based on these mechanisms, Wu *et al.* first reported a stretchable temperature sensor based on PAM/carrageenan DN hydrogel in 2018, which displayed a sensitivity as high as  $2.6\%/^\circ\text{C}$  at an extreme tensile strain of 200%.<sup>124</sup> Then, they found that the dehydration treatment of the hydrogel can further improve its thermal sensing ability, that is, the increased temperature can lead to a greater resistance change due to the better blocking and

trapping of ions caused by the dehydrated high-density polymer network at room temperature.<sup>277</sup> Meanwhile, the organohydrogel thus evolved can also achieve ultra-sensitive temperature detection ( $19.6\% \text{ }^\circ\text{C}^{-1}$ ) and a wide detection range (0–102  $^\circ\text{C}$ ), which is attributed to the higher initial resistance, smaller heat capacity, and stronger hydrogen bonds formed between organic molecules and water molecules in the organohydrogel. Among various flexible materials, organohydrogels neither freeze at sub-zero temperatures like hydrogels nor dissolve at higher temperatures like organogels, which makes them a good material for manufacturing temperature sensors. In consideration of these, various flexible temperature sensors based on organohydrogels have been developed,<sup>91,132</sup> but their thermal sensitivity still needs further breakthroughs.

Humidity and gas sensors also have important practical significance, but they have rarely been reported in flexible devices made of intrinsically stretchable materials. Humidity and gas have a standard concentration in the production and living environment; beyond this range, human health will be threatened. In addition, they are also important biomarkers in human exhaled breath and are closely related to human health.<sup>261</sup> Therefore, the development of stretchable organohydrogel-based wearable humidity or gas sensors is of great significance to medicine. And the real-time monitoring of humidity and gas can not only prevent but also diagnose diseases. The response of organohydrogels to humidity is mainly related to changes in the concentration and mobility of charge carriers caused by the physical or chemical adsorption of water molecules in the gel network. Wu *et al.* fabricated highly sensitive humidity sensors by using intrinsically ultrastretchable k-carrageenan/PAM organohydrogels.<sup>63</sup> The high response of this organohydrogel to humidity is attributed to the formation of hydrogen bonds between water molecules and a large number of hydrophilic groups in the gel network, including  $-\text{OH}$  and  $\text{SO}_3^-$  on k-carrageenan,  $-\text{NH}_2$  on PAM, and abundant  $-\text{OH}$  on organic molecules (Fig. 15). Impressively, the incorporation of organic agents not only boosts the sensitivity by increasing the adsorption sites, but also improves the long-term stability and detection range due to the enhanced moisture-holding ability of the organohydrogel, demonstrating the advantages of organohydrogels in fabricating stretchable humidity sensors. Subsequently, Wu *et al.* showed that this organohydrogel can also detect  $\text{NH}_3$  and  $\text{NO}_2$  due to the effective adsorption of gas molecules on the abundant functional groups of the gel network.<sup>278</sup> This organohydrogel gas sensor exhibited high sensitivity ( $8.4$  and  $1.4 \text{ ppm}^{-1}$  for  $\text{NO}_2$  and  $\text{NH}_3$ , respectively) and ultralow theoretical limit of detection ( $91.6$  and  $3.5 \text{ ppb}$  for  $\text{NH}_3$  and  $\text{NO}_2$ , respectively) at room temperature without thermal or light activation, which has obvious advantages compared with other types of traditional gas sensors (such as graphene, reduced graphene oxide (rGO), MXene, metal oxide, *etc.*), resulting in low energy consumption and better safety. The in-depth gas sensing mechanism of ion-conducting hydrogel/organohydrogel may also relate to the redox reactions that occurred at the gel-electrode interface,<sup>279,280</sup> which requires further investigation. Considering that humidity and gas sensing



**Fig. 15** The humidity sensing performance and mechanism of an organohydrogel. (a) Dynamic response curves of the DN hydrogel and EG/Gly-DN organohydrogels to different humidity ranging from 90% to 24% RH. (b) Dynamic response curves of the Gly-DN organohydrogel to lower humidity ranging from 24% to 4% RH. (c) Relationship between the humidity and responses of these sensors. (d) Repeatability test, (e) response–recovery curve and (f) long-term stability of the Gly-DN organohydrogel-based sensor to human respiration. (g–i) Schematic diagram of the sensing mechanism of an organohydrogel to humidity, the response is mainly related to the formation of hydrogen bonds between water molecules and the hydrophilic groups on carrageenan and PAM, promoting moisture adsorption. Reproduced with permission.<sup>63</sup> Copyright 2019, Royal Society of Chemistry.

are mainly related to surface reactions, the development of some micro/nanostructures with a higher specific surface area (such as a three-dimensional structure) is an important strategy for improving the sensitivity of organohydrogels to gas or humidity, which can be investigated in the near future.

#### 4.2. Energy storage devices

Electrochemical energy storage devices have attracted much attention due to the energy crisis and the increasing demand for sustainable energy, mainly including supercapacitors and metal-ion batteries.<sup>5,281</sup> The traditional structure of energy storage devices mainly includes electrodes, electrolytes, and current collectors. Metal-ion batteries realize energy storage and release through the intercalation and de-intercalation of metal ions between the positive and negative electrodes. Reversible electrochemical reactions occur on the surface and inside of the electrodes during the charge and discharge process,<sup>282,283</sup> while supercapacitors mainly rely on the electrostatic adsorption and desorption of electrolyte ions on the electrode surface or the occurrence of reversible redox reactions to achieve charge storage and release.<sup>284,285</sup> Nowadays, the development of flexible energy storage devices is imperative, which is conducive to reducing their mechanical damage, increasing their service life and serving as a power supply unit for wearable devices. Its realization requires the cooperation of various components. However, traditional electrode materials

such as activated carbon and transition metal composites<sup>286</sup> are rigid powders and lack flexibility. New electrode materials, including CNTs, carbon fibers, graphene, and conductive polymers,<sup>287–289</sup> have both considerable electrochemical properties and varying degrees of flexibility, making it possible to realize flexible electrodes.

The traditional liquid electrolyte is volatile, flammable, and easy to leak under mechanical external force, resulting in poor safety and unsatisfactory long-term stability of the device. Therefore, more attention has recently been paid to the development of solid-state polymer electrolytes. Generally, the solid-state polymer electrolyte needs to have sufficient ionic conductivity and good mechanical properties to achieve flexible energy storage devices with better electrochemical performance. In some instances, good frost resistance, thermal stability, and flame retardancy should be achieved in the solid-state polymer electrolyte to enable it to work in harsh environments. It is obvious that simple hydrogels cannot meet these requirements due to their own limitations, and the addition of ionic liquids to the hydrogels will correspondingly cause higher costs and toxicity.<sup>44,84,85,290–295</sup> Satisfactorily, organohydrogels show great advantages to prepare all-temperature flexible electrolytes due to their excellent anti-freezing and moisturizing ability. Nevertheless, the lower ionic conductivity of the organohydrogel electrolytes compared to that of the liquid electrolytes will lead to high equivalent series resistance (ESR) and subsequent low power output, which is not conducive to their practical applications. Considering this, the ionic conductivity of the organohydrogel electrolyte is generally improved by adding some metal salt.

Among various polymers, PVA has good mechanical properties and hydrophilicity; it is currently the most common polymer for preparing organohydrogel electrolytes due to its high adsorption capacity of electrolytes and low commercial price.<sup>296–299</sup> For example, Rong *et al.* reported a low temperature tolerant PVA-based organohydrogel electrolyte by using the water/EG binary solvent.<sup>42</sup> The high ionic conductivity ( $2.38 \text{ mS cm}^{-1}$  at  $-40 \text{ }^\circ\text{C}$ ) of the organohydrogel electrolyte was achieved by adding LiCl as the electrolyte salt. Additionally, Lu and Chen constructed a flexible supercapacitor with high energy density and long cycling life based on an anti-freezing and thermally stable montmorillonite (MMT)/PVA organohydrogel electrolyte.<sup>300</sup> This device can not only deliver a stable energy supply under bending, twisting, and stretching states, but also exhibit good mechanical and electrochemical properties under a wide temperature range from  $-50$  to  $90 \text{ }^\circ\text{C}$  (Fig. 16). Specifically, lamellar structural MMT materials are not only employed as flame retardants due to the strong hydrogen bond formation with PVA chains, but also increase the ionic conductivity by providing oriented channels in the PVA matrix for more efficient ion migration. Considering the relatively weak hydrogen bond interaction in PVA gel, Liu *et al.* demonstrated a thermally stable and anti-freezing organohydrogel synthesized by the copolymerization of AM and 2-acrylamido-2-methylpropane sulfonic acid (AMPS) in a water/DMSO binary solvent system containing LiCl conductive additives,<sup>301</sup> which is a promising candidate to be used as an electrolyte for flexible

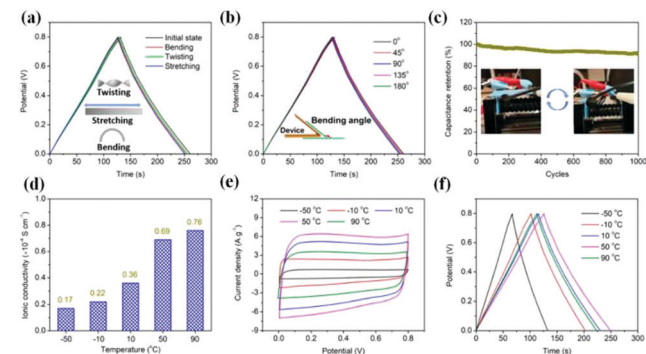


**Fig. 16** Stability of flexible supercapacitors based on an organohydrogel electrolyte. Galvanostatic charge–discharge (GCD) curves of the device (a) under different flexible conditions and (b) under different bending angles. (c) Bending tests of flexible supercapacitors. (d) Ionic conductivity, (e) cyclic voltammogram (CV) curves and (f) GCD curves of the device under different operation temperatures. Reproduced with permission.<sup>300</sup> Copyright 2020, American Chemical Society.

supercapacitors with high electrochemical performance and wide temperature adaptability. Meanwhile, the resulting supercapacitors also exhibited excellent flexibility and mechanically bending stability. Likewise, benefiting from the excellent mechanical properties and exceptional freeze resistance of the organohydrogel electrolyte, a freeze-resistant flexible zinc manganese-dioxide battery constructed by sandwiching an EG based waterborne anionic polyurethane acrylate (EG-waPUA)/PAM organohydrogel electrolyte containing  $2 \text{ mol L}^{-1} \text{ ZnSO}_4$  and  $0.1 \text{ mol L}^{-1} \text{ MnSO}_4$  between the fabricated flexible zinc anode and  $\alpha\text{-MnO}_2/\text{CNT}$  cathode was also developed.<sup>118</sup> As a result, this solid-state battery still exhibits good electrochemical performance at sub-zero temperatures or under various deformations, owing to the outstanding flexibility and conductive stability.

Furthermore, the undesirable electrochemical performance of the device can also be attributed to insufficient interface contact between the electrode material and the gel electrolyte, and these interfaces may partially detach after long-term cycling or at low temperatures due to their different thermal expansion coefficients. To address this problem, Wang *et al.* designed an all-in-one supercapacitor by infusing the PVA-KOH organohydrogel electrolyte into the 3D multiwall carbon nanotube (MWCNT) network as electrodes,<sup>302</sup> which exhibited superior capacitive behavior at sub-zero temperatures and excellent cycling performance due to the stable electrode–electrolyte interfaces. Also, it showed a good mechanical performance due to the synergistic effect of flexible electrolytes and MWCNTs. Hou *et al.* reported a flexible solid supercapacitor by combining the rGO electrode with the PVA-based organohydrogel electrolyte without the usage of binders;<sup>148</sup> the excellent flexibility and good electrochemical performance of the organohydrogel electrolyte even at low temperature enable this device to be used in harsh environments. The good contact between the electrode and the organohydrogel electrolyte stems from the excellent self-adhesiveness of the organohydrogel, ensuring lower interfacial resistance and better electrochemical stability of this supercapacitor. Additionally, the flexibility of the rGO electrode is

greatly increased by heating the GO membranes to form a honeycomb-like porous microstructure, thereby achieving the overall flexibility of the device. Although these flexible energy storage devices have been successfully implemented, their electrochemical performance is still unsatisfactory when compared with those of the traditional ones, and needs to be improved in the future.

### 4.3. Nanogenerator

The self-powered ability is a promising strategy to solve the current problem of continuous energy supply of wearable and implantable electronic devices, which shows great practical significance. Considering the sensing and energy storage capabilities of organohydrogels, a self-powered sensing system integrating strain sensors and supercapacitors was proposed by Huang *et al.*<sup>303,304</sup> In these cases, the strain sensor was powered by the supercapacitor, and the sensing materials and electrolytes in the system were composed of the same ionic organohydrogel. Although the output voltage of the supercapacitor and the sensor was gradually decreasing due to the self-discharge behavior, the resistance change caused by the applied strain remained unchanged, showing a stable sensor output. More importantly, thanks to the excellent mechanical flexibility and wide environmental tolerance of the organohydrogel, this integrated system can be directly attached to the human body to detect human movement without external power supply under various environments. However, the supercapacitor still requires an additional charging process, which is not conducive to the sustainable use of the device. In comparison, nanogenerators can realize continuous energy supply by converting mechanical, light, heat, and chemical energy into electrical energy, which is currently the main research focus for constructing self-powered devices.<sup>305</sup>

Nowadays, flexible triboelectric nanogenerator (TENG) based on the occurrence of triboelectricity between various materials with different electron affinity and electrostatic induction (Fig. 17a) is considered to be a promising power supply for wearable electronics through the harvest of biomechanical energy.<sup>306</sup> Hydrogels have been widely used in wearable TENG due to their ultrahigh stretchability, excellent conductivity, good self-healing capability, and adhesion abilities that can be imparted, which are conducive to their direct attachment to organisms and prevent various mechanical impacts during operation, but they cannot work stably as the environment changes.<sup>295,307</sup> In this context, TENG constructed using organohydrogel as the electrode layer shows an excellent environmental tolerance and stability and has significant advantages in practical applications. For example, Sun *et al.* prepared a sustainable TENG using a conductive nanocomposite organohydrogel as the electrode material, which could effectively collect mechanical energy from human activities within a wide temperature range ( $-60$  to  $60$  °C), with a maximum output power density of  $41.2 \text{ mW m}^{-2}$ .<sup>66</sup> The resulting TENG could be connected with various capacitors to build a self-charging power system and directly power different portable electronics. Huang *et al.* reported a sandwich structured TENG constructed by two

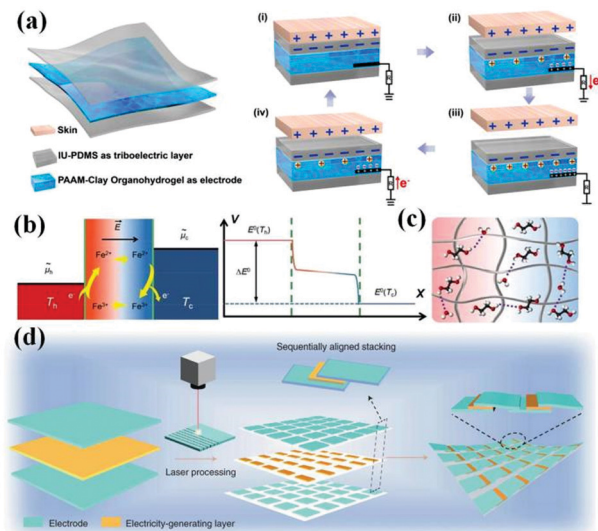


**Fig. 17** The mechanism of an organohydrogel-based nanogenerator and the corresponding scalable integration method. (a) Schematic diagram of the structure and electricity generation mechanism of the organohydrogel-based TENG. Reproduced with permission.<sup>308</sup> Copyright 2021, Elsevier. (b) Schematic diagram of the thermoelectric effect of the organohydrogel with the addition of  $\text{Fe}^{3+/2+}$  redox ions. (c) Structure diagram of organic hydrogel under temperature gradient. Reproduced with permission.<sup>310</sup> Copyright 2021, John Wiley and Sons. (d) Schematic diagram of a sequentially aligned stacking method that integrates nanogenerator units in series. Reproduced with permission.<sup>311</sup> Copyright 2021, Springer Nature.

IU-PDMS membranes and a single PAM-clay organohydrogel layer, which exhibited a maximum output power density of  $710 \text{ mW m}^{-2}$ .<sup>308</sup> Compared with the hydrogel-based TENG, the output performance of this obtained TENG was very stable in a wide temperature range ( $-30$  to  $80$  °C), thanks to the ultra-fast self-healing ability and excellent environment tolerance of the organohydrogel. Since the open-circuit voltage ( $V_{oc}$ ) of TENG is related to the contact area between tribomaterials, this TENG can be exploited as a self-powered sensor to detect different human motion modes. Notably, the output performance of TENG is positively related to the ionic conductivity in organohydrogel. To this end, Wu *et al.* developed a single-electrode TENG based on DN ionic conductive organohydrogels, which can maintain a stable output in a broad temperature range from  $-50$  to  $100$  °C and after four months of storage, showing excellent environmental stability.<sup>309</sup> These organohydrogels can maintain a stable charge channel after solvent replacement because more ions can be bonded to the polymer chains of the DN through dipole interactions and stronger sodium bonds can be formed through electrostatic interaction, which subsequently results in a higher conductivity and output power density ( $1.02$ – $1.81 \text{ W m}^{-2}$ ).

Beyond that, energy harvesting technology that converts the abundant green energy in nature into electricity is equally important in the sustainable energy supply. For example, thermoelectric materials based on the Seebeck effect can realize the conversion of heat to electricity so as to maintain the continuous operation of electronic devices.<sup>312</sup> Taking into

account the poor mechanical flexibility of traditional inorganic thermoelectric materials, organohydrogels added with thermogalvanic ions have greater advantages in the preparation of environmentally tolerant flexible thermoelectric generators. Gao *et al.* designed a stretchable organohydrogel thermocell, which can still maintain relatively good thermoelectric performance even at sub-zero temperatures and has the potential to be used in polar and space exploration.<sup>310</sup> In this case, a relatively high power density ( $0.1 \text{ mW m}^{-2} \text{ K}^{-2}$ ) was achieved by adding the redox couple of  $\text{Fe}^{3+/2+}$  as thermogalvanic ions and methyl chloride quaternized *N,N*-dimethylamino ethylacrylate (DMAEA-Q) as a chaotropic comonomer. As shown in Fig. 17b and c, the reduction of  $\text{Fe}^{3+}$  at the high-temperature electrode and the oxidation of  $\text{Fe}^{2+}$  at the low-temperature electrode could cause a difference in the electrode potential on both sides of the organohydrogel, resulting in a voltage output. Subsequently, the consumption of iron ions at one electrode can lead to the diffusion and replenishment of the same ions on the other side, realizing the continuous power supply of this system. DMAEA-Q can promote the increase of the entropy difference of redox ions by combining with  $\text{Fe}^{3+}$  and thus enhance the thermoelectric effect. Furthermore, the moist-electric generator also has huge application potential as an energy supply. He *et al.* utilized organohydrogels to realize the conversion of ambient moisture to electricity, with an output voltage of  $80 \text{ mV}$  under constant moisture flow.<sup>16</sup> In detail, the electrical output is due to the release of protons produced by the dissociation of the hydroxyl groups on the side close to the humid air and the movement of these protons to the other side driven by the concentration gradient. Equally important, given the small output voltage of these generators, their scalable integration is essential for the realization of power supply for electronic devices in practice. For instance, a sequentially aligned stacking method was developed to integrate the moist-electric generator unit on various flexible substrates by laser processing (Fig. 17d).<sup>311</sup> The integrated device formed by 1600 units in series could achieve a high output voltage of  $1000 \text{ V}$ , demonstrating the feasibility of nanogenerators in practice.

#### 4.4. Biomedicine

An organohydrogel is an ideal material for wearable dressing or wound dressing due to its flexibility and adaptability. Considering the advantages of good adhesiveness and anti-freezing ability, an organohydrogel can serve as an excellent wearable dressing to protect skin from frostbite.<sup>84</sup> Meanwhile, imparting ultraviolet (UV)-blocking capabilities to organohydrogel dressings can protect human skin from exposure to UV radiation that may induce skin cancer,<sup>313</sup> which is also important in other wearable electronic devices. Therefore, a PVA-TA@talc organohydrogel with remarkable UV-filtering capabilities was prepared, owing to the UV reflection of talc and the UV absorption of TA in the organohydrogel.<sup>71</sup> Sun *et al.* also prepared a PVA-based organohydrogel with UV blocking capabilities by adding TA, demonstrating the effectiveness of TA in absorbing and shielding UV light.<sup>73</sup>

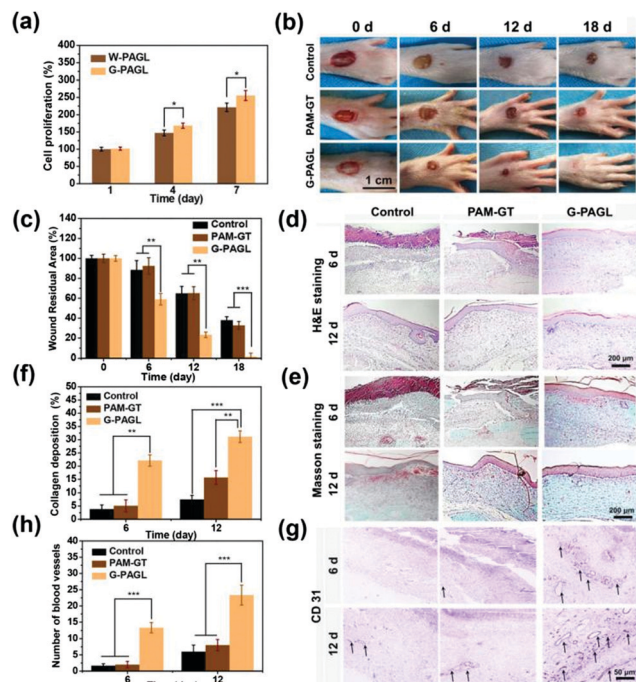


**Fig. 18** An organohydrogel for wound dressing. (a) Cell proliferation of L929 cells in W-PAGL (hydrogel) and G-PAGL (organohydrogel) for different days. The therapeutic effects of the phosphate-buffered saline (PBS, control), PAM-GT hydrogel, and G-PAGL (organohydrogel) on infectious DFUs: (b) representative photographs and (c) quantification of the wound residual area at different time points. (d) Characterization of granulation tissue formation at the wound site by hematoxylin and eosin (H&E) staining. (e) Characterization of the newly formed collagen deposition in the regenerated skin tissue by Masson's trichrome staining and (f) the corresponding quantification of collagen deposition percentage *via* measuring the intensity of the blue-stained areas. (g) Characterization of neovascularization in granulation tissue *via* CD31 immunohistochemical staining and (h) the corresponding quantification of blood vessels. The wound healing process treated with an organohydrogel produces more granulation tissue, collagen deposition and new blood vessels, showing better wound healing effectiveness. Reproduced with permission.<sup>53</sup> Copyright 2021, American Chemical Society.

Wound dressings are widely used in clinics. At present, the traditional wound dressings commonly used in the market are usually gauze, bandages, or sponges, and they usually only have the function of forming a physical barrier and absorbing tissue exudate. However, in addition to these basic functions, an ideal wound dressing also needs to have excellent antibacterial ability to prevent infection or inflammation and maintain high humidity at the wound surface to facilitate the regeneration of wound granulation tissue and epithelial cells and subsequently promote wound healing.<sup>314–316</sup> In addition, wound dressing should exhibit good adaptability to biological tissues and self-adhesiveness so that it can meet the healing requirements of different wounds and cannot cause secondary damage to the wound during the removal process. To date, various wound dressings based on hydrogels cross-linked by different biocompatible polymers (such as PVA,<sup>317,318</sup> PAM,<sup>85,319</sup> and chitosan<sup>320,321</sup>) have been studied. However, the hydrogel is easy to dry in the air, leading to the loss of various properties

and even damaging the wound. Significantly, organohydrogels can mimic biological tissues well due to their high softness, elasticity, and water content similar to that of tissues, and the specific functional design can impart them with high self-adhesiveness, antibacterial properties, and admirable biocompatibility. More importantly, the unique moisturizing ability and frost resistance of organohydrogel can extend the service life of the corresponding wound dressing and broaden its application environment, making it more suitable as a wound dressing material. Note that most organic cryoprotectants are harmful to organisms, Gly has good biocompatibility and cannot cause secondary damage to wounds. Driven by this, Liu *et al.* utilized a water/Gly binary solvent to fabricate organohydrogels containing PAM, gelatin, and non-biotoxic antibacterial  $\epsilon$ -PL chains.<sup>53</sup> This organohydrogel exhibited excellent mechanical properties, high adhesiveness, and good antibacterial properties in a wide temperature range ( $-20$  to  $60$  °C), which could efficiently promote the healing of diabetic foot ulcers (DFUs) by inducing cell proliferation, accelerating collagen deposition, promoting angiogenesis, and inhibiting bacterial breed as a wound dressing (Fig. 18).

Based on the above discussion, organohydrogels can be well used to construct various flexible devices by imparting corresponding functionality. However, when considering the application of these devices in practice, the performance and stability of the devices are the most important, which need to be continuously optimized in subsequent research studies. Simultaneously, the application of organohydrogels in some new fields should be explored.

## 5. Conclusions and outlook

In this review, we summarized recent developments of organohydrogels from various aspects, including preparation strategies, performance optimization, and applications. Owing to their unique anti-freezing and water retention ability, solvent resistance, adjustable surface wettability, and shape memory effect, organohydrogels are ideal candidates for the preparation of flexible devices that can operate under various harsh conditions or be used in intelligent systems. In addition, organohydrogels can be easily endowed with various functionalities due to the reconfigurable polymer network structure, which is conducive to more flexible and stable applications. Considering these excellent electro-mechanical properties and various functionalities in organohydrogels, they have been widely applied in sensors, energy storage devices, nanogenerators, and biomedical fields.

Although great progress has been made in the development of organohydrogels and related devices, a huge gap still exists compared with the research history of inorganic materials such as metals or semiconductors. Many challenges still need to be addressed in the future research of organohydrogels:

First of all, the current diversity and synthesis techniques of organohydrogels are still insufficient, mainly limited by the solubility of organic substances and the elusive polymerization



conditions; more simple and unrestricted preparation methods for different organohydrogels need to be developed. In particular, organohydrogels with different polymer networks urgently need to be developed so as to achieve some fascinating intrinsic properties. For example, fluorine-rich polymers can exist stably in strong acids and alkalis due to the high electronegativity of fluorine, so they can be used for developing organohydrogels with wide pH adaptability. Also, these polymers can impart good self-healing ability to the resulting organohydrogels.

Secondly, current flexible devices are mainly constructed based on bulk materials, which limits their large-scale integration. In particular, the preparation of micro-/nano-sized or microstructured organohydrogels also plays an important role in the optimization of their properties. Furthermore, the miniaturization and integration of organohydrogels are quite necessary for their development in flexible integrated electronics, but they are currently rarely involved due to their poor controllability. Recently, 3D printing technology has made good progress in patterning and miniaturization of hydrogels, and it is conceivable that it will also be dedicated to the development of miniaturized organohydrogels.

Thirdly, although good freezing resistance and moisturizing ability are realized in organohydrogels, their environmental tolerance still needs to be further optimized. At sub-zero temperatures, the crystallization of water molecules in the organohydrogel is well prevented, but the freezing of water molecules adsorbed on the surface still occurs. Therefore, surface hydrophobic treatment becomes indispensable in the preparation process of an organohydrogel. In addition, dehydration still inevitably occurs especially after size reduction due to the exposure of the more specific surface area.

Fourthly, in addition to maintaining structural integrity, it is equally important and more challenging to achieve functional stability of organohydrogels in various environments, such as underwater adhesion and self-healing at sub-zero temperatures. Thus, more stable adhesion or self-healing mechanisms need to be developed and used in organohydrogels. Also, the various properties of the organohydrogels require further optimization. For example, the decrease in conductivity of organohydrogels synthesized by solvent replacement needs to be addressed in the future. Moreover, considering the limited functionality of current organohydrogels due to the dilemma between some properties, a prominent organohydrogel with multiple functions is expected to be developed in the future based on functionality balance.

Fifthly, although organohydrogels have been proven to be applied in various fields, device performance and stability still need to be further improved. Interestingly, some organohydrogels also show great potential to be developed and applied to smart materials, oil-water separation, or underwater electronics, and their feasibility needs further verification. Moreover, lots of efforts can be put into the full use of organohydrogels and the development of multifunctional integrated systems with lower costs.

Finally, the current *in situ* characterization methods have made great progress, such as Raman spectroscopy, infrared spectroscopy, electrochemical impedance spectroscopy, *etc.*

Correspondingly, these will enable more in-depth mechanism exploration of organohydrogels under different behaviors that are not completely clear.

## Author contributions

Q. L. Ding: conceptualization, methodology, investigation, writing – original draft, and review & editing. Z. X. Wu: conceptualization, investigation, and writing – review & editing. K. Tao, W. Y. Wang, Y. M. Wei, B. R. Yang, and X. Xie: writing – review & editing. J. Wu: conceived this research, supervision, investigation, writing – original draft, and review & editing.

## Conflicts of interest

There are no conflicts to declare.

## Acknowledgements

J. W. acknowledges financial support from the National Natural Science Foundation of China (61801525), the Guangdong Basic and Applied Basic Research Foundation (2020A1515010693), and the Science and Technology Program of Guangzhou (201904010456).

## Notes and references

- 1 C. Yang and Z. Suo, *Nat. Rev. Mater.*, 2018, **3**, 125–142.
- 2 E. M. Ahmed, *J. Adv. Res.*, 2015, **6**, 105–121.
- 3 J. Y. Sun, C. Keplinger, G. M. Whitesides and Z. Suo, *Adv. Mater.*, 2014, **26**, 7608–7614.
- 4 Z. Wu, X. Yang and J. Wu, *ACS Appl. Mater. Interfaces*, 2021, **13**, 2128–2144.
- 5 X. Tong, Z. Tian, J. Sun, V. Tung, R. B. Kaner and Y. Shao, *Mater. Today*, 2021, **44**, 78.
- 6 S. Xia, Y. Chen, J. Tian, J. Shi, C. Geng, H. Zou, M. Liang and Z. Li, *Adv. Funct. Mater.*, 2021, 2101143.
- 7 H. E. Jeong, S. H. Lee, P. Kim and K. Y. Suh, *Nano Lett.*, 2006, **6**, 1508–1513.
- 8 H. Liu, J. Gao, W. Huang, K. Dai, G. Zheng, C. Liu, C. Shen, X. Yan, J. Guo and Z. Guo, *Nanoscale*, 2016, **8**, 12977–12989.
- 9 Y. Yang, G. Zhao, X. Cheng, H. Deng and Q. Fu, *ACS Appl. Mater. Interfaces*, 2021, **13**, 14599–14611.
- 10 Y. Ma, Y. Yu, P. She, J. Lu, S. Liu, W. Huang and Q. Zhao, *Sci. Adv.*, 2020, **6**, eaaz2386.
- 11 Y. Jian, S. Handschuh-Wang, J. Zhang, W. Lu, X. Zhou and T. Chen, *Mater. Horiz.*, 2021, **8**, 351–369.
- 12 N. A. Peppas, J. Z. Hilt, A. Khademhosseini and R. Langer, *Adv. Mater.*, 2006, **18**, 1345–1360.
- 13 T. R. Hoare and D. S. Kohane, *Polymer*, 2008, **49**, 1993–2007.
- 14 H. Yuk, S. Lin, C. Ma, M. Takaffoli, N. X. Fang and X. Zhao, *Nat. Commun.*, 2017, **8**, 1–12.
- 15 Y. Yang, L. Guan, X. Li, Z. Gao, X. Ren and G. Gao, *ACS Appl. Mater. Interfaces*, 2018, **11**, 3428–3437.
- 16 P. He, J. Wu, X. Pan, L. Chen, K. Liu, H. Gao, H. Wu, S. Cao, L. Huang and Y. Ni, *J. Mater. Chem. A*, 2020, **8**, 3109–3118.

- 17 M. K. Jaiswal, J. R. Xavier, J. K. Carrow, P. Desai, D. Alge and A. K. Gaharwar, *ACS Nano*, 2015, **10**, 246–256.
- 18 M. Hua, S. Wu, Y. Ma, Y. Zhao, Z. Chen, I. Frenkel, J. Strzalka, H. Zhou, X. Zhu and X. He, *Nature*, 2021, **590**, 594–599.
- 19 X.-J. Zha, S.-T. Zhang, J.-H. Pu, X. Zhao, K. Ke, R.-Y. Bao, L. Bai, Z.-Y. Liu, M.-B. Yang and W. Yang, *ACS Appl. Mater. Interfaces*, 2020, **12**, 23514–23522.
- 20 G. Chen, J. Huang, J. Gu, S. Peng, X. Xiang, K. Chen, X. Yang, L. Guan, X. Jiang and L. Hou, *J. Mater. Chem. A*, 2020, **8**, 6776–6784.
- 21 W. Xue, M. B. Huglin and E. Khoshdel, *Polym. Int.*, 1999, **48**, 8–14.
- 22 K.-T. Huang, K. Ishihara and C.-J. Huang, *Biomacromolecules*, 2019, **20**, 3524–3534.
- 23 Y. Wei, L. Xiang, H. Ou, F. Li, Y. Zhang, Y. Qian, L. Hao, J. Diao, M. Zhang and P. Zhu, *Adv. Funct. Mater.*, 2020, **30**, 2005135.
- 24 X. P. Morelle, W. R. Illeperuma, K. Tian, R. Bai, Z. Suo and J. J. Vlassak, *Adv. Mater.*, 2018, **30**, 1801541.
- 25 S. Li, L. Wang, W. Zheng, G. Yang and X. Jiang, *Adv. Funct. Mater.*, 2020, **30**, 2002370.
- 26 X. Liu, Q. Zhang, L. Duan and G. Gao, *ACS Appl. Mater. Interfaces*, 2019, **11**, 6644–6651.
- 27 Y. Ma, J. Yao, Q. Liu, T. Han, J. Zhao, X. Ma, Y. Tong, G. Jin, K. Qu and B. Li, *Adv. Funct. Mater.*, 2020, **30**, 2001820.
- 28 M. Lo Presti, G. Rizzo, G. M. Farinola and F. G. Omenetto, *Adv. Sci.*, 2021, 2004786.
- 29 N. D. Catron, H. Lee and P. B. Messersmith, *Biointerphases*, 2006, **1**, 134–141.
- 30 L.-D. Koh, Y. Cheng, C.-P. Teng, Y.-W. Khin, X.-J. Loh, S.-Y. Tee, M. Low, E. Ye, H.-D. Yu and Y.-W. Zhang, *Prog. Polym. Sci.*, 2015, **46**, 86–110.
- 31 C. Zhong, T. Gurry, A. A. Cheng, J. Downey, Z. Deng, C. M. Stultz and T. K. Lu, *Nat. Nanotechnol.*, 2014, **9**, 858–866.
- 32 S. M. Roopan and D. Devipriya, *Polymer Gels*, Springer, 2018, pp. 285–310.
- 33 Y. Gao, L. Shi, S. Lu, T. Zhu, X. Da, Y. Li, H. Bu, G. Gao and S. Ding, *Chem. Mater.*, 2019, **31**, 3257–3264.
- 34 J. Ryu, S. H. Ku, H. Lee and C. B. Park, *Adv. Funct. Mater.*, 2010, **20**, 2132–2139.
- 35 A. Wang, Y. Wang, B. Zhang, K. Wan, J. Zhu, J. Xu, C. Zhang and T. Liu, *Chem. Eng. J.*, 2021, **411**, 128506.
- 36 Z. Wang, Y. Cong and J. Fu, *J. Mater. Chem. B*, 2020, **8**, 3437–3459.
- 37 T. Zhao, G. Wang, D. Hao, L. Chen, K. Liu and M. Liu, *Adv. Funct. Mater.*, 2018, **28**, 1800793.
- 38 C. Wang, K. Hu, C. Zhao, Y. Zou, Y. Liu, X. Qu, D. Jiang, Z. Li, M. R. Zhang and Z. Li, *Small*, 2020, **16**, 1904758.
- 39 D. Zhou, F. Chen, S. Handschuh-Wang, T. Gan, X. Zhou and X. Zhou, *ChemPhysChem*, 2019, **20**, 2139–2154.
- 40 T. Wang, Y. Zhang, Q. Liu, W. Cheng, X. Wang, L. Pan, B. Xu and H. Xu, *Adv. Funct. Mater.*, 2018, **28**, 1705551.
- 41 Y. Guo and S. Dong, *Anal. Chem.*, 1997, **69**, 1904–1908.
- 42 Q. Rong, W. Lei, J. Huang and M. Liu, *Adv. Energy Mater.*, 2018, **8**, 1801967.
- 43 X. Su, H. Wang, Z. Tian, X. Duan, Z. Chai, Y. Feng, Y. Wang, Y. Fan and J. Huang, *ACS Appl. Mater. Interfaces*, 2020, **12**, 29757–29766.
- 44 H. Gao, Z. Zhao, Y. Cai, J. Zhou, W. Hua, L. Chen, L. Wang, J. Zhang, D. Han and M. Liu, *Nat. Commun.*, 2017, **8**, 1–8.
- 45 X. Liu, Q. Zhang and G. Gao, *ACS Nano*, 2020, **14**, 13709–13717.
- 46 Z. Zhao, C. Li, Z. Dong, Y. Yang, L. Zhang, S. Zhuo, X. Zhou, Y. Xu, L. Jiang and M. Liu, *Adv. Funct. Mater.*, 2019, **29**, 1807858.
- 47 Z. Zhao, K. Zhang, Y. Liu, J. Zhou and M. Liu, *Adv. Mater.*, 2017, **29**, 1701695.
- 48 J. Chen, Q. Dong, X. Ma, T.-H. Fan and Y. Lei, *Sci. Rep.*, 2016, **6**, 1–9.
- 49 Q. Rong, W. Lei, L. Chen, Y. Yin, J. Zhou and M. Liu, *Angew. Chem., Int. Ed.*, 2017, **56**, 14159–14163.
- 50 R. Ricciardi, F. Auriemma, C. Gaillet, C. De Rosa and F. Lauprêtre, *Macromolecules*, 2004, **37**, 9510–9516.
- 51 J. Y. Chang, D. Godovsky, M. Han, C. Hassan, J. Kim, B. Lee, Y. Lee, N. Peppas, R. Quirk and T. Yoo, *Biopolymers-PVA Hydrogels Anionic Polymerisation Nanocomposites*, Springer Science & Business Media, 2000.
- 52 X.-J. Zha, S.-T. Zhang, J.-H. Pu, X. Zhao, K. Ke, R.-Y. Bao, L. Bai, Z.-Y. Liu, M.-B. Yang and W. Yang, *ACS Appl. Mater. Interfaces*, 2020, **12**, 23514–23522.
- 53 H. Liu, Z. Li, Y. Zhao, Y. Feng, A. V. Zvyagin, J. Wang, X. Yang, B. Yang and Q. Lin, *ACS Appl. Mater. Interfaces*, 2021, **13**, 26770–26781.
- 54 L. Guo, R. H. Colby, C. P. Lusignan and T. H. Whitesides, *Macromolecules*, 2003, **36**, 9999–10008.
- 55 Z. Qin, D. Dong, M. Yao, Q. Yu, X. Sun, Q. Guo, H. Zhang, F. Yao and J. Li, *ACS Appl. Mater. Interfaces*, 2019, **11**, 21184–21193.
- 56 B. Jeong, S. W. Kim and Y. H. Bae, *Adv. Drug Delivery Rev.*, 2012, **64**, 154–162.
- 57 R. Yoshida, *Adv. Mater.*, 2010, **22**, 3463–3483.
- 58 K. Murata, M. Aoki, T. Suzuki, T. Harada, H. Kawabata, T. Komori, F. Ohseto, K. Ueda and S. Shinkai, *J. Am. Chem. Soc.*, 1994, **116**, 6664–6676.
- 59 C. T. Lee, K. A. Smith and T. A. Hatton, *Macromolecules*, 2004, **37**, 5397–5405.
- 60 I. Tomatsu, A. Hashidzume and A. Harada, *J. Am. Chem. Soc.*, 2006, **128**, 2226–2227.
- 61 S. Ahmed, X. Sallenave, F. Fages and G. Mieden-Gundert, *Langmuir*, 2002, **18**, 7096–7101.
- 62 S.-i. Kawano, N. Fujita and S. Shinkai, *J. Am. Chem. Soc.*, 2004, **126**, 8592–8593.
- 63 J. Wu, Z. Wu, H. Xu, Q. Wu, C. Liu, B.-R. Yang, X. Gui, X. Xie, K. Tao and Y. Shen, *Mater. Horiz.*, 2019, **6**, 595–603.
- 64 Z. He and W. Yuan, *ACS Appl. Mater. Interfaces*, 2021, **13**, 1474–1485.
- 65 X. Wan, X. Xu, X. Liu, L. Jia, X. He and S. Wang, *Adv. Mater.*, 2021, **33**, 2008557.
- 66 H. Sun, Y. Zhao, S. Jiao, C. Wang, Y. Jia, K. Dai, G. Zheng, C. Liu, P. Wan and C. Shen, *Adv. Funct. Mater.*, 2021, **31**, 2101696.

- 67 J. Liu, Z. Chen, Y. Chen, H. U. Rehman, Y. Guo, H. Li and H. Liu, *Adv. Funct. Mater.*, 2021, **31**, 2101464.
- 68 X. Sui, H. Guo, C. Cai, Q. Li, C. Wen, X. Zhang, X. Wang, J. Yang and L. Zhang, *Chem. Eng. J.*, 2021, **419**, 129478.
- 69 K. Wang, J. Wang, L. Li, L. Xu, N. Feng, Y. Wang, X. Fei, J. Tian and Y. Li, *Chem. Eng. J.*, 2019, **372**, 216–225.
- 70 X. Wu, H. Liao, D. Ma, M. Chao, Y. Wang, X. Jia, P. Wan and L. Zhang, *J. Mater. Chem. C*, 2020, **8**, 1788–1795.
- 71 X. Pan, Q. Wang, R. Guo, Y. Ni, K. Liu, X. Ouyang, L. Chen, L. Huang, S. Cao and M. Xie, *J. Mater. Chem. A*, 2019, **7**, 4525–4535.
- 72 G. Ge, Y.-Z. Zhang, W. Zhang, W. Yuan, J. K. El-Demellawi, P. Zhang, E. Di Fabrizio, X. Dong and H. N. Alshareef, *ACS Nano*, 2021, **15**, 2698–2706.
- 73 C. Sun, C. Hou, H. Zhang, Y. Li, Q. Zhang and H. Wang, *APL Mater.*, 2021, **9**, 011101.
- 74 J. Song, S. Chen, L. Sun, Y. Guo, L. Zhang, S. Wang, H. Xuan, Q. Guan and Z. You, *Adv. Mater.*, 2020, **32**, 1906994.
- 75 K. Tian, J. Bae, S. E. Bakarich, C. Yang, R. D. Gately, G. M. Spinks, M. in het Panhuis, Z. Suo and J. J. Vlassak, *Adv. Mater.*, 2017, **29**, 1604827.
- 76 H. Liu, W. Zhao, G. Gao and X. Ren, *Mater. Today Commun.*, 2019, **21**, 100609.
- 77 M. Amjadi, A. Pichitpajongkit, S. Lee, S. Ryu and I. Park, *ACS Nano*, 2014, **8**, 5154–5163.
- 78 J. Chen and E. Dickinson, *Colloids Surf., B*, 1999, **12**, 373–381.
- 79 T. B. Blijdenstein, W. P. Hendriks, E. van der Linden, T. van Vliet and G. A. van Aken, *Langmuir*, 2003, **19**, 6657–6663.
- 80 S. Zhuo, Z. Zhao, Z. Xie, Y. Hao, Y. Xu, T. Zhao, H. Li, E. M. Knubben, L. Wen and L. Jiang, *Sci. Adv.*, 2020, **6**, eaax1464.
- 81 C. Li, S. Feng, C. Li, Y. Sui, J. Shen, C. Huang, Y. Wu and W. Huang, *Adv. Funct. Mater.*, 2020, **30**, 2002163.
- 82 Y. Liu, L. Wang, H. Lu and Z. Huang, *Langmuir*, 2021, **37**, 6711.
- 83 S. Shi, X. Peng, T. Liu, Y.-N. Chen, C. He and H. Wang, *Polymer*, 2017, **111**, 168–176.
- 84 L. Han, K. Liu, M. Wang, K. Wang, L. Fang, H. Chen, J. Zhou and X. Lu, *Adv. Funct. Mater.*, 2018, **28**, 1704195.
- 85 F. Chen, D. Zhou, J. Wang, T. Li, X. Zhou, T. Gan, S. Handschuh-Wang and X. Zhou, *Angew. Chem.*, 2018, **130**, 6678–6681.
- 86 J. W. Zhang, D. D. Dong, X. Y. Guan, E. M. Zhang, Y. M. Chen, K. Yang, Y. X. Zhang, M. M. B. Khan, Y. Arfat and Y. Aziz, *Front. Chem.*, 2020, **8**, 102.
- 87 J. Wu, Z. Wu, X. Lu, S. Han, B.-R. Yang, X. Gui, K. Tao, J. Miao and C. Liu, *ACS Appl. Mater. Interfaces*, 2019, **11**, 9405–9414.
- 88 L. Fang, J. Zhang, W. Wang, Y. Zhang, F. Chen, J. Zhou, F. Chen, R. Li, X. Zhou and Z. Xie, *ACS Appl. Mater. Interfaces*, 2020, **12**, 56393–56402.
- 89 M. Matsugami, T. Takamuku, T. Otomo and T. Yamaguchi, *J. Phys. Chem. B*, 2006, **110**, 12372–12379.
- 90 W. P. Williams, P. J. Quinn, L. I. Tsonev and R. D. Koynova, *Biochim. Biophys. Acta, Biomembr.*, 1991, **1062**, 123–132.
- 91 J. Gu, J. Huang, G. Chen, L. Hou, J. Zhang, X. Zhang, X. Yang, L. Guan, X. Jiang and H. Liu, *ACS Appl. Mater. Interfaces*, 2020, **12**, 40815–40827.
- 92 D. Rasmussen and A. MacKenzie, *Nature*, 1968, **220**, 1315–1317.
- 93 J. F. Abrahamsen, A. M. Bakken and Ø. Bruserud, *Transfusion*, 2002, **42**, 1573–1580.
- 94 X. Zhao, F. Chen, Y. Li, H. Lu, N. Zhang and M. Ma, *Nat. Commun.*, 2018, **9**, 1–8.
- 95 Y. Ye, Y. Zhang, Y. Chen, X. Han and F. Jiang, *Adv. Funct. Mater.*, 2020, **30**, 2003430.
- 96 S. Cervený, J. Colmenero and A. Alegria, *Macromolecules*, 2005, **38**, 7056–7063.
- 97 H. Kiani and D.-W. Sun, *Trends Food Sci. Technol.*, 2011, **22**, 407–426.
- 98 H. Yuk, T. Zhang, G. A. Parada, X. Liu and X. Zhao, *Nat. Commun.*, 2016, **7**, 1–11.
- 99 X. Liu, Q. Zhang, L. Duan and G. Gao, *Adv. Funct. Mater.*, 2019, **29**, 1900450.
- 100 Y.-Q. Wang, Y. Zhu, J.-H. Wang, X.-N. Li, X.-G. Wu, Y.-X. Qin and W.-Y. Chen, *Compos. Sci. Technol.*, 2021, **206**, 108653.
- 101 B. Q. Y. Chan, Z. W. K. Low, S. J. W. Heng, S. Y. Chan, C. Owh and X. J. Loh, *ACS Appl. Mater. Interfaces*, 2016, **8**, 10070–10087.
- 102 Y. Wong, J. Kong, L. K. Widjaja and S. S. Venkatraman, *Sci. China: Chem.*, 2014, **57**, 476–489.
- 103 G. Li, G. Fei, H. Xia, J. Han and Y. Zhao, *J. Mater. Chem.*, 2012, **22**, 7692–7696.
- 104 R. Liang, L. Wang, H. Yu, A. Khan, B. U. Amin and R. U. Khan, *Eur. Polym. J.*, 2019, **114**, 380–396.
- 105 C.-H. Lu, W. Guo, Y. Hu, X.-J. Qi and I. Willner, *J. Am. Chem. Soc.*, 2015, **137**, 15723–15731.
- 106 Y. Liu, H. Du, L. Liu and J. Leng, *Smart Mater. Struct.*, 2014, **23**, 023001.
- 107 H. Meng and G. Li, *Polymer*, 2013, **54**, 2199–2221.
- 108 Y. Zhang, J. Liao, T. Wang, W. Sun and Z. Tong, *Adv. Funct. Mater.*, 2018, **28**, 1707245.
- 109 J. G. Hardy, M. Palma, S. J. Wind and M. J. Biggs, *Adv. Mater.*, 2016, **28**, 5717–5724.
- 110 A. T. Neffe, B. D. Hanh, S. Steuer and A. Lendlein, *Adv. Mater.*, 2009, **21**, 3394–3398.
- 111 T. Xie, *Polymer*, 2011, **52**, 4985–5000.
- 112 W. Voit, T. Ware, R. R. Dasari, P. Smith, L. Danz, D. Simon, S. Barlow, S. R. Marder and K. Gall, *Adv. Funct. Mater.*, 2010, **20**, 162–171.
- 113 N. Zheng, G. Fang, Z. Cao, Q. Zhao and T. Xie, *Polym. Chem.*, 2015, **6**, 3046–3053.
- 114 Y. Osada and A. Matsuda, *Nature*, 1995, **376**, 219–219.
- 115 J. Hao and R. Weiss, *ACS Macro Lett.*, 2013, **2**, 86–89.
- 116 Y. Zhang, Y. Li and W. Liu, *Adv. Funct. Mater.*, 2015, **25**, 471–480.
- 117 Z. Zhao, S. Zhuo, R. Fang, L. Zhang, X. Zhou, Y. Xu, J. Zhang, Z. Dong, L. Jiang and M. Liu, *Adv. Mater.*, 2018, **30**, 1804435.
- 118 F. Mo, G. Liang, Q. Meng, Z. Liu, H. Li, J. Fan and C. Zhi, *Energy Environ. Sci.*, 2019, **12**, 706–715.

- 119 S. Bao, J. Gao, T. Xu, N. Li, W. Chen and W. Lu, *Chem. Eng. J.*, 2021, **411**, 128470.
- 120 W. Zheng, L. Xu, Y. Li, Y. Huang, B. Li, Z. Jiang and G. Gao, *J. Colloid Interface Sci.*, 2021, **594**, 584–592.
- 121 Z. Qin, X. Sun, H. Zhang, Q. Yu, X. Wang, S. He, F. Yao and J. Li, *J. Mater. Chem. A*, 2020, **8**, 4447–4456.
- 122 J.-Y. Sun, X. Zhao, W. R. Illeperuma, O. Chaudhuri, K. H. Oh, D. J. Mooney, J. J. Vlassak and Z. Suo, *Nature*, 2012, **489**, 133–136.
- 123 L. Fang, Z. Cai, Z. Ding, T. Chen, J. Zhang, F. Chen, J. Shen, F. Chen, R. Li and X. Zhou, *ACS Appl. Mater. Interfaces*, 2019, **11**, 21895–21903.
- 124 J. Wu, S. Han, T. Yang, Z. Li, Z. Wu, X. Gui, K. Tao, J. Miao, L. K. Norford and C. Liu, *ACS Appl. Mater. Interfaces*, 2018, **10**, 19097–19105.
- 125 G. Ramorino, F. Bignotti, S. Pandini and T. Riccò, *Compos. Sci. Technol.*, 2009, **69**, 1206–1211.
- 126 T. Bai, B. Zhu, H. Liu, Y. Wang, G. Song, C. Liu and C. Shen, *Int. J. Biol. Macromol.*, 2020, **151**, 628–634.
- 127 O. Lourie, D. Cox and H. Wagner, *Phys. Rev. Lett.*, 1998, **81**, 1638.
- 128 J. Y. Kim, *Materials*, 2009, **2**, 1955–1974.
- 129 J. H. Xu, S. Ye, C. Di Ding, L. H. Tan and J. J. Fu, *J. Mater. Chem. A*, 2018, **6**, 5887–5898.
- 130 X. Gong, J. Liu, S. Baskaran, R. D. Voise and J. S. Young, *Chem. Mater.*, 2000, **12**, 1049–1052.
- 131 M. K. Jaiswal, J. R. Xavier, J. K. Carrow, P. Desai, D. Alge and A. K. Gaharwar, *ACS Nano*, 2016, **10**, 246–256.
- 132 G. Ge, Y. Lu, X. Qu, W. Zhao, Y. Ren, W. Wang, Q. Wang, W. Huang and X. Dong, *ACS Nano*, 2019, **14**, 218–228.
- 133 S. Wu, M. Hua, Y. Alsaïd, Y. Du, Y. Ma, Y. Zhao, C. Y. Lo, C. Wang, D. Wu and B. Yao, *Adv. Mater.*, 2021, **33**, 2007829.
- 134 P. Lin, S. Ma, X. Wang and F. Zhou, *Adv. Mater.*, 2015, **27**, 2054–2059.
- 135 P. Lin, T. Zhang, X. Wang, B. Yu and F. Zhou, *Small*, 2016, **12**, 4386–4392.
- 136 C. Xiang, Z. Wang, C. Yang, X. Yao, Y. Wang and Z. Suo, *Mater. Today*, 2020, **34**, 7–16.
- 137 H. Zhang, I. Hussain, M. Brust, M. F. Butler, S. P. Rannard and A. I. Cooper, *Nat. Mater.*, 2005, **4**, 787–793.
- 138 M. T. I. Mredha, H. H. Le, P. Trtik, J. Cui and I. Jeon, *Mater. Horiz.*, 2019, **6**, 1504–1511.
- 139 M. T. I. Mredha, Y. Z. Guo, T. Nonoyama, T. Nakajima, T. Kurokawa and J. P. Gong, *Adv. Mater.*, 2018, **30**, 1704937.
- 140 Y. Huang, D. R. King, T. L. Sun, T. Nonoyama, T. Kurokawa, T. Nakajima and J. P. Gong, *Adv. Funct. Mater.*, 2017, **27**, 1605350.
- 141 X. Hu, M. Vatankhah-Varnoosfaderani, J. Zhou, Q. Li and S. S. Sheiko, *Adv. Mater.*, 2015, **27**, 6899–6905.
- 142 Q. He, Y. Huang and S. Wang, *Adv. Funct. Mater.*, 2018, **28**, 1705069.
- 143 R. Bai, J. Yang, X. P. Morelle and Z. Suo, *Macromol. Rapid Commun.*, 2019, **40**, 1800883.
- 144 C. N. Maganaris and J. P. Paul, *J. Physiol.*, 1999, **521**, 307.
- 145 C. Keplinger, J.-Y. Sun, C. C. Foo, P. Rothemund, G. M. Whitesides and Z. Suo, *Science*, 2013, **341**, 984–987.
- 146 H. R. Lee, C. C. Kim and J. Y. Sun, *Adv. Mater.*, 2018, **30**, 1704403.
- 147 C. Liu, S. Han, H. Xu, J. Wu and C. Liu, *ACS Appl. Mater. Interfaces*, 2018, **10**, 31716–31724.
- 148 X. Hou, Q. Zhang, L. Wang, G. Gao and W. Lü, *ACS Appl. Mater. Interfaces*, 2021, **13**, 12432–12441.
- 149 H. Chen, X. Ren and G. Gao, *ACS Appl. Mater. Interfaces*, 2019, **11**, 28336–28344.
- 150 Y. Shi, L. Pan, B. Liu, Y. Wang, Y. Cui, Z. Bao and G. Yu, *J. Mater. Chem. A*, 2014, **2**, 6086–6091.
- 151 D. Mawad, E. Stewart, D. L. Officer, T. Romeo, P. Wagner, K. Wagner and G. G. Wallace, *Adv. Funct. Mater.*, 2012, **22**, 2692–2699.
- 152 Y. Zhao, B. Liu, L. Pan and G. Yu, *Energy Environ. Sci.*, 2013, **6**, 2856–2870.
- 153 S. Naficy, J. M. Razal, G. M. Spinks, G. G. Wallace and P. G. Whitten, *Chem. Mater.*, 2012, **24**, 3425–3433.
- 154 C. Wang, S. Wang, G. Chen, W. Kong, W. Ping, J. Dai, G. Pastel, H. Xie, S. He and S. Das, *Chem. Mater.*, 2018, **30**, 7707–7713.
- 155 T. Li, S. X. Li, W. Kong, C. Chen, E. Hitz, C. Jia, J. Dai, X. Zhang, R. Briber and Z. Siwy, *Sci. Adv.*, 2019, **5**, eaau4238.
- 156 X. Tian, Y. Yi, P. Yang, P. Liu, L. Qu, M. Li, Y.-s. Hu and B. Yang, *ACS Appl. Mater. Interfaces*, 2019, **11**, 4001–4010.
- 157 H. Liu, X. Chen, Y. Zheng, D. Zhang, Y. Zhao, C. Wang, C. Pan, C. Liu and C. Shen, *Adv. Funct. Mater.*, 2021, **31**, 2008006.
- 158 S. Sharma, A. Chhetry, S. Zhang, H. Yoon, C. Park, H. Kim, M. Sharifuzzaman, X. Hui and J. Y. Park, *ACS Nano*, 2021, **15**, 4380–4393.
- 159 K. Maleski, V. N. Mochalin and Y. Gogotsi, *Chem. Mater.*, 2017, **29**, 1632–1640.
- 160 B. J. Blaiszik, S. L. Kramer, S. C. Olugebefola, J. S. Moore, N. R. Sottos and S. R. White, *Annu. Rev. Mater. Res.*, 2010, **40**, 179–211.
- 161 Y. Huang, M. Zhu, Y. Huang, Z. Pei, H. Li, Z. Wang, Q. Xue and C. Zhi, *Adv. Mater.*, 2016, **28**, 8344–8364.
- 162 Y. Yang and M. W. Urban, *Chem. Soc. Rev.*, 2013, **42**, 7446–7467.
- 163 M. Q. Zhang and M. Z. Rong, *J. Polym. Sci., Part B: Polym. Phys.*, 2012, **50**, 229–241.
- 164 X. He, C. Zhang, M. Wang, Y. Zhang, L. Liu and W. Yang, *ACS Appl. Mater. Interfaces*, 2017, **9**, 11134–11143.
- 165 Y. Cao, T. G. Morrissey, E. Acome, S. I. Allec, B. M. Wong, C. Keplinger and C. Wang, *Adv. Mater.*, 2017, **29**, 1605099.
- 166 H. Qin, T. Zhang, H.-N. Li, H.-P. Cong, M. Antonietti and S.-H. Yu, *Chem*, 2017, **3**, 691–705.
- 167 L. Shi, H. Carstensen, K. Hölzl, M. Lunzer, H. Li, J. Hilborn, A. Ovsianikov and D. A. Ossipov, *Chem. Mater.*, 2017, **29**, 5816–5823.
- 168 M. Burnworth, L. Tang, J. R. Kumpfer, A. J. Duncan, F. L. Beyer, G. L. Fiore, S. J. Rowan and C. Weder, *Nature*, 2011, **472**, 334–337.
- 169 Y. Guo, K. Zheng and P. Wan, *Small*, 2018, **14**, 1704497.
- 170 G. Li, H. Zhang, D. Fortin, H. Xia and Y. Zhao, *Langmuir*, 2015, **31**, 11709–11716.

- 171 M. Nakahata, Y. Takashima, H. Yamaguchi and A. Harada, *Nat. Commun.*, 2011, **2**, 1–6.
- 172 Q. Yang, P. Wang, C. Zhao, W. Wang, J. Yang and Q. Liu, *Macromol. Rapid Commun.*, 2017, **38**, 1600741.
- 173 Z. Wang, Y. Ren, Y. Zhu, L. Hao, Y. Chen, G. An, H. Wu, X. Shi and C. Mao, *Angew. Chem.*, 2018, **130**, 9146–9150.
- 174 Y. Shi, M. Wang, C. Ma, Y. Wang, X. Li and G. Yu, *Nano Lett.*, 2015, **15**, 6276–6281.
- 175 M. A. Darabi, A. Khosrozadeh, R. Mbeleck, Y. Liu, Q. Chang, J. Jiang, J. Cai, Q. Wang, G. Luo and M. Xing, *Adv. Mater.*, 2017, **29**, 1700533.
- 176 P. Cordier, F. Tournilhac, C. Soulié-Ziakovic and L. Leibler, *Nature*, 2008, **451**, 977–980.
- 177 D. C. Tuncaboylu, A. Argun, M. Sahin, M. Sari and O. Okay, *Polymer*, 2012, **53**, 5513–5522.
- 178 V. Can, Z. Kochovski, V. Reiter, N. Severin, M. Siebenbürger, B. Kent, J. Just, J. r. P. Rabe, M. Ballauff and O. Okay, *Macromolecules*, 2016, **49**, 2281–2287.
- 179 Y. Ren, R. Lou, X. Liu, M. Gao, H. Zheng, T. Yang, H. Xie, W. Yu and X. Ma, *Chem. Commun.*, 2016, **52**, 6273–6276.
- 180 M. W. England, C. Urata, G. J. Dunderdale and A. Hozumi, *ACS Appl. Mater. Interfaces*, 2016, **8**, 4318–4322.
- 181 Y. Xu, Q. Wu, Y. Sun, H. Bai and G. Shi, *ACS Nano*, 2010, **4**, 7358–7362.
- 182 A. J. Patil, J. L. Vickery, T. B. Scott and S. Mann, *Adv. Mater.*, 2009, **21**, 3159–3164.
- 183 S. Burattini, B. W. Greenland, W. Hayes, M. E. Mackay, S. J. Rowan and H. M. Colquhoun, *Chem. Mater.*, 2011, **23**, 6–8.
- 184 H. Guo, Y. J. Tan, G. Chen, Z. Wang, G. J. Susanto, H. H. See, Z. Yang, Z. W. Lim, L. Yang and B. C. Tee, *Nat. Commun.*, 2020, **11**, 1–10.
- 185 G. E. Fantner, E. Oroudjev, G. Schitter, L. S. Golde, P. Thurner, M. M. Finch, P. Turner, T. Gutschmann, D. E. Morse and H. Hansma, *Biophys. J.*, 2006, **90**, 1411–1418.
- 186 F.-Y. Hsieh, H.-W. Han, X.-R. Chen, C.-S. Yang, Y. Wei and S.-H. Hsu, *Biomaterials*, 2018, **174**, 31–40.
- 187 F.-Y. Hsieh, L. Tao, Y. Wei and S.-H. Hsu, *NPG Asia Mater.*, 2017, **9**, e363–e363.
- 188 C. e. Yuan, M. Z. Rong, M. Q. Zhang, Z. P. Zhang and Y. C. Yuan, *Chem. Mater.*, 2011, **23**, 5076–5081.
- 189 G. Deng, F. Li, H. Yu, F. Liu, C. Liu, W. Sun, H. Jiang and Y. Chen, *ACS Macro Lett.*, 2012, **1**, 275–279.
- 190 P. Casuso, I. Odriozola, A. N. Pérez-San Vicente, I. Loinaz, G. N. Cabañero, H.-J. R. Grande and D. Dupin, *Biomacromolecules*, 2015, **16**, 3552–3561.
- 191 Z. Liu, Y. Wang, Y. Ren, G. Jin, C. Zhang, W. Chen and F. Yan, *Mater. Horiz.*, 2020, **7**, 919–927.
- 192 D. L. Taylor and M. in het Panhuis, *Adv. Mater.*, 2016, **28**, 9060–9093.
- 193 W.-P. Chen, D.-Z. Hao, W.-J. Hao, X.-L. Guo and L. Jiang, *ACS Appl. Mater. Interfaces*, 2018, **10**, 1258–1265.
- 194 V. K. Thakur and M. R. Kessler, *Polymer*, 2015, **69**, 369–383.
- 195 B. J. Kim, D. X. Oh, S. Kim, J. H. Seo, D. S. Hwang, A. Masic, D. K. Han and H. J. Cha, *Biomacromolecules*, 2014, **15**, 1579–1585.
- 196 Q. Lu, E. Danner, J. H. Waite, J. N. Israelachvili, H. Zeng and D. S. Hwang, *J. R. Soc., Interface*, 2013, **10**, 20120759.
- 197 S. A. Burke, M. Ritter-Jones, B. P. Lee and P. B. Messersmith, *Biomed. Mater.*, 2007, **2**, 203.
- 198 N. Holten-Andersen, A. Jaishankar, M. J. Harrington, D. E. Fullenkamp, G. DiMarco, L. He, G. H. McKinley, P. B. Messersmith and K. Y. C. Lee, *J. Mater. Chem. B*, 2014, **2**, 2467–2472.
- 199 T. Yamada, Y. Hayamizu, Y. Yamamoto, Y. Yomogida, A. Izadi-Najafabadi, D. N. Futaba and K. Hata, *Nat. Nanotechnol.*, 2011, **6**, 296–301.
- 200 H. Yuk, T. Zhang, S. Lin, G. A. Parada and X. Zhao, *Nat. Mater.*, 2016, **15**, 190–196.
- 201 H. Zhou, J. Lai, X. Jin, H. Liu, X. Li, W. Chen, A. Ma and X. Zhou, *Chem. Eng. J.*, 2021, **413**, 127544.
- 202 J. Xu, R. Jin, X. Ren and G. Gao, *Chem. Eng. J.*, 2021, **413**, 127446.
- 203 J. Tang, J. Li, J. J. Vlassak and Z. Suo, *Soft Matter*, 2016, **12**, 1093–1099.
- 204 Q. Liu, G. Nian, C. Yang, S. Qu and Z. Suo, *Nat. Commun.*, 2018, **9**, 1–11.
- 205 L. Zhou, C. Dai, L. Fan, Y. Jiang, C. Liu, Z. Zhou, P. Guan, Y. Tian, J. Xing and X. Li, *Adv. Funct. Mater.*, 2021, **31**, 2007457.
- 206 G. Ye, J. Qiu, X. Fang, T. Yu, Y. Xie, Y. Zhao, D. Yan, C. He and N. Liu, *Mater. Horiz.*, 2021, **8**, 1047–1057.
- 207 Y. Niu, H. Liu, R. He, M. Luo, M. Shu and F. Xu, *Small*, 2021, **17**, 2101151.
- 208 H. Zhou, J. Lai, B. Zheng, X. Jin, G. Zhao, H. Liu, W. Chen, A. Ma, X. Li and Y. Wu, *Adv. Funct. Mater.*, 2021, 2108423.
- 209 S. Lim, Y. S. Choi, D. G. Kang, Y. H. Song and H. J. Cha, *Biomaterials*, 2010, **31**, 3715–3722.
- 210 Y. Chen, J. Meng, Z. Gu, X. Wan, L. Jiang and S. Wang, *Adv. Funct. Mater.*, 2020, **30**, 1905287.
- 211 J. H. Waite, N. H. Andersen, S. Jewhurst and C. Sun, *J. Adhes.*, 2005, **81**, 297–317.
- 212 T. Priemel, E. Degtyar, M. N. Dean and M. J. Harrington, *Nat. Commun.*, 2017, **8**, 1–12.
- 213 X. Pei, J. Wang, Y. Cong and J. Fu, *J. Polym. Sci.*, 2021, **59**, 1312.
- 214 S. Wu, Z. Zhao, J. R. Rzasa, E. Kim, J. Li, E. VanArsdale, W. E. Bentley, X. Shi and G. F. Payne, *Adv. Funct. Mater.*, 2021, **31**, 2007709.
- 215 C. Zhang, B. Wu, Y. Zhou, F. Zhou, W. Liu and Z. Wang, *Chem. Soc. Rev.*, 2020, **49**, 3605–3637.
- 216 L. Han, M. Wang, P. Li, D. Gan, L. Yan, J. Xu, K. Wang, L. Fang, C. W. Chan and H. Zhang, *ACS Appl. Mater. Interfaces*, 2018, **10**, 28015–28026.
- 217 L. Han, L. Yan, K. Wang, L. Fang, H. Zhang, Y. Tang, Y. Ding, L.-T. Weng, J. Xu and J. Weng, *NPG Asia Mater.*, 2017, **9**, e372–e372.
- 218 H. Ejima, J. J. Richardson, K. Liang, J. P. Best, M. P. van Koeveden, G. K. Such, J. Cui and F. Caruso, *Science*, 2013, **341**, 154–157.
- 219 T. S. Sileika, D. G. Barrett, R. Zhang, K. H. A. Lau and P. B. Messersmith, *Angew. Chem.*, 2013, **125**, 10966–10970.

- 220 D. X. Oh, S. Kim, D. Lee and D. S. Hwang, *Acta Biomater.*, 2015, **20**, 104–112.
- 221 A. S. Lee, P. J. Mahon and D. C. Creagh, *Vib. Spectrosc.*, 2006, **41**, 170–175.
- 222 H. Kumari, S. R. Kline, C. L. Dennis, A. V. Mossine, R. L. Paul, C. A. Deakne and J. L. Atwood, *Angew. Chem.*, 2012, **124**, 9397–9400.
- 223 J. P. McManus, K. G. Davis, J. E. Beart, S. H. Gaffney, T. H. Lilley and E. Haslam, *J. Chem. Soc., Perkin Trans. 2*, 1985, 1429–1438.
- 224 K. Kustin, S. Liu, C. Nicolini and D. Toppen, *J. Am. Chem. Soc.*, 1974, **96**, 7410–7415.
- 225 G. Huber, H. Mantz, R. Spolenak, K. Mecke, K. Jacobs, S. N. Gorb and E. Arzt, *Proc. Natl. Acad. Sci. U. S. A.*, 2005, **102**, 16293–16296.
- 226 A. L. Urzedo, M. C. Gonçalves, M. H. Nascimento, C. B. Lombello, G. Nakazato and A. B. Seabra, *ACS Biomater. Sci. Eng.*, 2020, **6**, 2117–2134.
- 227 A. Y. Gahane, V. Singh, A. Kumar and A. K. Thakur, *Biomater. Sci.*, 2020, **8**, 1996–2006.
- 228 H. Ji, H. Sun and X. Qu, *Adv. Drug Delivery Rev.*, 2016, **105**, 176–189.
- 229 G. He, X. Chen, Y. Yin, W. Cai, W. Ke, Y. Kong and H. Zheng, *J. Biomater. Sci., Polym. Ed.*, 2016, **27**, 370–384.
- 230 S. Li, S. Dong, W. Xu, S. Tu, L. Yan, C. Zhao, J. Ding and X. Chen, *Adv. Sci.*, 2018, **5**, 1700527.
- 231 P. AshaRani, G. Low Kah Mun, M. P. Hande and S. Valiyaveetil, *ACS Nano*, 2009, **3**, 279–290.
- 232 J. He, M. Shi, Y. Liang and B. Guo, *Chem. Eng. J.*, 2020, **394**, 124888.
- 233 M. Li, X. Liu, L. Tan, Z. Cui, X. Yang, Z. Li, Y. Zheng, K. W. K. Yeung, P. K. Chu and S. Wu, *Biomater. Sci.*, 2018, **6**, 2110–2121.
- 234 Z. Zhao, R. Yan, X. Yi, J. Li, J. Rao, Z. Guo, Y. Yang, W. Li, Y.-Q. Li and C. Chen, *ACS Nano*, 2017, **11**, 4428–4438.
- 235 M. Baumgartner, F. Hartmann, M. Drack, D. Preninger, D. Wirthl, R. Gerstmayr, L. Lehner, G. Mao, R. Pruckner and S. Demchyshyn, *Nat. Mater.*, 2020, **19**, 1102–1109.
- 236 L. Feng, W. Shi, Q. Chen, H. Cheng, J. Bao, C. Jiang, W. Zhao and C. Zhao, *Adv. Healthcare Mater.*, 2021, 2100784.
- 237 X. Zhang, L.-Y. Xia, X. Chen, Z. Chen and F.-G. Wu, *Sci. China Mater.*, 2017, **60**, 487–503.
- 238 Z. Yang, R. Huang, B. Zheng, W. Guo, C. Li, W. He, Y. Wei, Y. Du, H. Wang and D. Wu, *Adv. Sci.*, 2021, **8**, 2003627.
- 239 X. Zhao, B. Guo, H. Wu, Y. Liang and P. X. Ma, *Nat. Commun.*, 2018, **9**, 1–17.
- 240 J. Qu, X. Zhao, Y. Liang, T. Zhang, P. X. Ma and B. Guo, *Biomaterials*, 2018, **183**, 185–199.
- 241 C. Wang, H. Niu, X. Ma, H. Hong, Y. Yuan and C. Liu, *ACS Appl. Mater. Interfaces*, 2019, **11**, 34595–34608.
- 242 Y. Su, L. Tian, M. Yu, Q. Gao, D. Wang, Y. Xi, P. Yang, B. Lei, P. X. Ma and P. Li, *Polym. Chem.*, 2017, **8**, 3788–3800.
- 243 Y. Zhang, L. Tao, S. Li and Y. Wei, *Biomacromolecules*, 2011, **12**, 2894–2901.
- 244 K. Zhang, J. L. Schnoor and E. Y. Zeng, *Environ. Sci. Technol.*, 2012, **46**, 10861–10867.
- 245 J. Wei, G. Wei, Y. Shang, J. Zhou, C. Wu and Q. Wang, *Adv. Mater.*, 2019, **31**, 1900248.
- 246 Y. Huang, M. Zhong, Y. Huang, M. Zhu, Z. Pei, Z. Wang, Q. Xue, X. Xie and C. Zhi, *Nat. Commun.*, 2015, **6**, 1–8.
- 247 Y. Huang, J. Liu, J. Wang, M. Hu, F. Mo, G. Liang and C. Zhi, *Angew. Chem., Int. Ed.*, 2018, **57**, 9810–9813.
- 248 Y. Guo, X. Zhou, Q. Tang, H. Bao, G. Wang and P. Saha, *J. Mater. Chem. A*, 2016, **4**, 8769–8776.
- 249 Y. Deng, Y. Zhang, B. Lemos and H. Ren, *Sci. Rep.*, 2017, **7**, 1–10.
- 250 V. R. Feig, H. Tran and Z. Bao, *ACS Cent. Sci.*, 2018, **4**, 337–348.
- 251 Z. Yu and P. Wu, *Adv. Mater.*, 2021, **33**, 2008479.
- 252 H. Shang, X. Le, M. Si, S. Wu, Y. Peng, F. Shan, S. Wu and T. Chen, *Chem. Eng. J.*, 2022, **429**, 132290.
- 253 X. Le, H. Shang, S. Wu, J. Zhang, M. Liu, Y. Zheng and T. Chen, *Adv. Funct. Mater.*, 2021, 2108365.
- 254 V. Solanki, S. Krupanidhi and K. Nanda, *ACS Appl. Mater. Interfaces*, 2017, **9**, 41428–41434.
- 255 P. M. Faia and C. S. Furtado, *Sens. Actuators, B*, 2013, **181**, 720–729.
- 256 J. Qi, S. Gao, K. Chen, J. Yang, H. Zhao, L. Guo and S. Yang, *J. Mater. Chem. A*, 2015, **3**, 18019–18026.
- 257 L. Liu, M. Ikram, L. Ma, X. Zhang, H. Lv, M. Ullah, M. Khan, H. Yu and K. Shi, *J. Hazard. Mater.*, 2020, **393**, 122325.
- 258 Z. Qin, K. Xu, H. Yue, H. Wang, J. Zhang, C. Ouyang, C. Xie and D. Zeng, *Sens. Actuators, B*, 2018, **262**, 771–779.
- 259 R. Kumar, W. Zheng, X. Liu, J. Zhang and M. Kumar, *Adv. Mater. Technol.*, 2020, **5**, 1901062.
- 260 N. Wang, M. Lin, H. Dai and H. Ma, *Biosens. Bioelectron.*, 2016, **79**, 320–326.
- 261 Y. Pang, J. Jian, T. Tu, Z. Yang, J. Ling, Y. Li, X. Wang, Y. Qiao, H. Tian and Y. Yang, *Biosens. Bioelectron.*, 2018, **116**, 123–129.
- 262 D. D. Han, Y. L. Zhang, J. N. Ma, Y. Liu, J. W. Mao, C. H. Han, K. Jiang, H. R. Zhao, T. Zhang and H. L. Xu, *Adv. Mater. Technol.*, 2017, **2**, 1700045.
- 263 H. Li, J. Chen, X. Chang, Y. Xu, G. Zhao, Y. Zhu and Y. Li, *J. Mater. Chem. A*, 2021, **9**, 1795–1802.
- 264 Y. Yang, G. Zhao, X. Cheng, H. Deng and Q. Fu, *ACS Appl. Mater. Interfaces*, 2021, **13**, 14599–14611.
- 265 G. Cai, J. Wang, K. Qian, J. Chen, S. Li and P. S. Lee, *Adv. Sci.*, 2017, **4**, 1600190.
- 266 W. Xu, J. Ma and E. Jabbari, *Acta Biomater.*, 2010, **6**, 1992–2002.
- 267 S. Han, C. Liu, X. Lin, J. Zheng, J. Wu and C. Liu, *ACS Appl. Polym. Mater.*, 2020, **2**, 996–1005.
- 268 R. Yu, C. Pan, J. Chen, G. Zhu and Z. L. Wang, *Adv. Funct. Mater.*, 2013, **23**, 5868–5874.
- 269 S. Gong, W. Schwalb, Y. Wang, Y. Chen, Y. Tang, J. Si, B. Shirinzadeh and W. Cheng, *Nat. Commun.*, 2014, **5**, 1–8.
- 270 M. Zhu, M. Lou, I. Abdalla, J. Yu, Z. Li and B. Ding, *Nano Energy*, 2020, **69**, 104429.

- 271 X. Wang, W.-Z. Song, M.-H. You, J. Zhang, M. Yu, Z. Fan, S. Ramakrishna and Y.-Z. Long, *ACS Nano*, 2018, **12**, 8588–8596.
- 272 M.-H. You, X.-X. Wang, X. Yan, J. Zhang, W.-Z. Song, M. Yu, Z.-Y. Fan, S. Ramakrishna and Y.-Z. Long, *J. Mater. Chem. A*, 2018, **6**, 3500–3509.
- 273 S. Lee, A. Reuveny, J. Reeder, S. Lee, H. Jin, Q. Liu, T. Yokota, T. Sekitani, T. Isoyama and Y. Abe, *Nat. Nanotechnol.*, 2016, **11**, 472–478.
- 274 C. Pang, G.-Y. Lee, T.-I. Kim, S. M. Kim, H. N. Kim, S.-H. Ahn and K.-Y. Suh, *Nat. Mater.*, 2012, **11**, 795–801.
- 275 Z. Wu, H. Ding, K. Tao, Y. Wei, X. Gui, W. Shi, X. Xie and J. Wu, *ACS Appl. Mater. Interfaces*, 2021, **13**, 21854–21864.
- 276 Z. Wu, W. Shi, H. Ding, B. Zhong, W. Huang, Y. Zhou, X. Gui, X. Xie and J. Wu, *J. Mater. Chem. C*, 2021, **9**, 13668–13679.
- 277 J. Wu, Z. Wu, Y. Wei, H. Ding, W. Huang, X. Gui, W. Shi, Y. Shen, K. Tao and X. Xie, *ACS Appl. Mater. Interfaces*, 2020, **12**, 19069–19079.
- 278 J. Wu, Z. Wu, W. Huang, X. Yang, Y. Liang, K. Tao, B.-R. Yang, W. Shi and X. Xie, *ACS Appl. Mater. Interfaces*, 2020, **12**, 52070–52081.
- 279 Z. Wu, L. Rong, J. Yang, Y. Wei, K. Tao, Y. Zhou, B. R. Yang, X. Xie and J. Wu, *Small*, 2021, 2104997.
- 280 Y. Liang, Z. Wu, Y. Wei, Q. Ding, K. Tao, X. Xie and J. Wu, *Nano-Micro Lett.*, 2022, **14**, 52.
- 281 H. Lin, S. Zhang, T. Zhang, H. Ye, Q. Yao, G. W. Zheng and J. Y. Lee, *Adv. Energy Mater.*, 2018, **8**, 1801868.
- 282 B. Dunn, H. Kamath and J.-M. Tarascon, *Science*, 2011, **334**, 928–935.
- 283 P. Guo, D. Liu, Z. Liu, X. Shang, Q. Liu and D. He, *Electrochim. Acta*, 2017, **256**, 28–36.
- 284 J. Chmiola, C. Largeot, P.-L. Taberna, P. Simon and Y. Gogotsi, *Science*, 2010, **328**, 480–483.
- 285 C. Lu and X. Chen, *J. Mater. Chem. A*, 2019, **7**, 20158–20161.
- 286 Z. Zhang, M. Liao, H. Lou, Y. Hu, X. Sun and H. Peng, *Adv. Mater.*, 2018, **30**, 1704261.
- 287 Y. Xu, Y. Zhang, Z. Guo, J. Ren, Y. Wang and H. Peng, *Angew. Chem.*, 2015, **127**, 15610–15614.
- 288 H. Jin, L. Zhou, C. L. Mak, H. Huang, W. M. Tang and H. L. W. Chan, *Nano Energy*, 2015, **11**, 662–670.
- 289 M. Kunitski, N. Eicke, P. Huber, J. Köhler, S. Zeller, J. Voigtsberger, N. Schlott, K. Henrichs, H. Sann and F. Trinter, *Nat. Commun.*, 2019, **10**, 1–7.
- 290 S. Wang, J. Xu, W. Wang, G.-J. N. Wang, R. Rastak, F. Molina-Lopez, J. W. Chung, S. Niu, V. R. Feig and J. Lopez, *Nature*, 2018, **555**, 83–88.
- 291 N. Chen, Y. Li, Y. Dai, W. Qu, Y. Xing, Y. Ye, Z. Wen, C. Guo, F. Wu and R. Chen, *J. Mater. Chem. A*, 2019, **7**, 9530–9536.
- 292 W. Wang, Y. Liu, S. Wang, X. Fu, T. Zhao, X. Chen and Z. Shao, *ACS Appl. Mater. Interfaces*, 2020, **12**, 25353–25362.
- 293 X. F. Zhang, X. Ma, T. Hou, K. Guo, J. Yin, Z. Wang, L. Shu, M. He and J. Yao, *Angew. Chem., Int. Ed.*, 2019, **58**, 7366–7370.
- 294 J. Le Bideau, L. Viau and A. Vioux, *Chem. Soc. Rev.*, 2011, **40**, 907–925.
- 295 L. Sun, S. Chen, Y. Guo, J. Song, L. Zhang, L. Xiao, Q. Guan and Z. You, *Nano Energy*, 2019, **63**, 103847.
- 296 Y. Yu, J. Zhong, W. Sun, R. Kumar and N. Koratkar, *Adv. Funct. Mater.*, 2017, **27**, 1606461.
- 297 C. Zhong, Y. Deng, W. Hu, J. Qiao, L. Zhang and J. Zhang, *Chem. Soc. Rev.*, 2015, **44**, 7484–7539.
- 298 C. Meng, C. Liu, L. Chen, C. Hu and S. Fan, *Nano Lett.*, 2010, **10**, 4025–4031.
- 299 W. Li, F. Gao, X. Wang, N. Zhang and M. Ma, *Angew. Chem.*, 2016, **128**, 9342–9347.
- 300 C. Lu and X. Chen, *Nano Lett.*, 2020, **20**, 1907–1914.
- 301 Y. Liu, H. Li, X. Wang, T. Lv, K. Dong, Z. Chen, Y. Yang, S. Cao and T. Chen, *J. Mater. Chem. A*, 2021, **9**, 12051–12059.
- 302 Y. Wang, H. Yuan, Y. Zhu, Z. Wang, Z. Hu, J. Xie, C. Liao, H. Cheng, F. Zhang and Z. Lu, *Sci. China Mater.*, 2020, **63**, 660–666.
- 303 J. Huang, S. Peng, J. Gu, G. Chen, J. Gao, J. Zhang, L. Hou, X. Yang, X. Jiang and L. Guan, *Mater. Horiz.*, 2020, **7**, 2085–2096.
- 304 J. Huang, J. Gu, J. Liu, J. Guo, H. Liu, K. Hou, X. Jiang, X. Yang and L. Guan, *J. Mater. Chem. A*, 2021, **9**, 16345–16358.
- 305 B. Sun, G. Zhou, K. Xu, Q. Yu and S. Duan, *ACS Mater. Lett.*, 2020, **2**, 1669–1690.
- 306 Y. Zou, V. Raveendran and J. Chen, *Nano Energy*, 2020, **77**, 105303.
- 307 K. Tao, Z. Chen, J. Yu, H. Zeng, J. Wu, Z. Wu, Q. Jia, P. Li, Y. Fu, H. Chang and W. Yuan, *Advanced Science*, 2022, 2104168.
- 308 L.-B. Huang, X. Dai, Z. Sun, M.-C. Wong, S.-Y. Pang, J. Han, Q. Zheng, C.-H. Zhao, J. Kong and J. Hao, *Nano Energy*, 2021, **82**, 105724.
- 309 Y. Wu, J. Qu, X. Zhang, K. Ao, Z. Zhou, Z. Zheng, Y. Mu, X. Wu, Y. Luo and S.-P. Feng, *ACS Nano*, 2021, **15**, 13427.
- 310 W. Gao, Z. Lei, C. Zhang, X. Liu and Y. Chen, *Adv. Funct. Mater.*, 2021, 2104071.
- 311 H. Wang, Y. Sun, T. He, Y. Huang, H. Cheng, C. Li, D. Xie, P. Yang, Y. Zhang and L. Qu, *Nat. Nanotechnol.*, 2021, **16**, 1–9.
- 312 J. Duan, G. Feng, B. Yu, J. Li, M. Chen, P. Yang, J. Feng, K. Liu and J. Zhou, *Nat. Commun.*, 2018, **9**, 1–8.
- 313 D. J. Moran and F. C. Hollows, *Br. J. Ophthalmol.*, 1984, **68**, 343–346.
- 314 D. Liang, Z. Lu, H. Yang, J. Gao and R. Chen, *ACS Appl. Mater. Interfaces*, 2016, **8**, 3958–3968.
- 315 Y. Hu, Z. Zhang, Y. Li, X. Ding, D. Li, C. Shen and F. J. Xu, *Macromol. Rapid Commun.*, 2018, **39**, 1800069.
- 316 M. Yin, X. Wang, Z. Yu, Y. Wang, X. Wang, M. Deng, D. Zhao, S. Ji, N. Jia and W. Zhang, *J. Mater. Chem. B*, 2020, **8**, 8395–8404.
- 317 H. Zhi, X. Fei, J. Tian, M. Jing, L. Xu, X. Wang, D. Liu, Y. Wang and J. Liu, *J. Mater. Chem. B*, 2017, **5**, 5738–5744.
- 318 H. Zhi, X. Fei, J. Tian, L. Zhao, H. Zhang, M. Jing, L. Xu, Y. Wang and Y. Li, *Biomater. Sci.*, 2018, **6**, 2320–2326.
- 319 W. J. Yang, X. Tao, T. Zhao, L. Weng, E.-T. Kang and L. Wang, *Polym. Chem.*, 2015, **6**, 7027–7035.
- 320 Z. Cao, X. Luo, H. Zhang, Z. Fu, Z. Shen, N. Cai, Y. Xue and F. Yu, *Cellulose*, 2016, **23**, 1349–1361.
- 321 K. Bankoti, A. P. Rameshababu, S. Datta, P. P. Maity, P. Goswami, P. Datta, S. K. Ghosh, A. Mitra and S. Dhara, *Mater. Sci. Eng., C*, 2017, **81**, 133–143.